European Journal of Medicinal Chemistry 183 (2019) 111676

Contents lists available at ScienceDirect

European Journal of Medicinal Chemistry

journal homepage: http://www.elsevier.com/locate/ejmech

Research paper

Discovery of a benzothiophene-flavonol halting miltefosine and antimonial drug resistance in *Leishmania* parasites through the application of medicinal chemistry, screening and genomics

Chiara Borsari [a, 1, 2], María Dolores Jiménez-Antón [b, c, 1], Julia Eick [d], Eugenia Bifeld [d], Juan José Torrado [b], Ana Isabel Olías-Molero [b, c], María Jesús Corral [b, c], Nuno Santarem [e], Catarina Baptista [e], Leda Severi [a], Sheraz Gul [f], Markus Wolf [f], Maria Kuzikov [f], Bernhard Ellinger [f], Jeanette Reinshagen [f], Gesa Witt [f], Pasquale Linciano [a], Annalisa Tait [a], Luca Costantino [a], Rosaria Luciani [a], Paloma Tejera Nevado [d], Dorothea Zander-Dinse [d], Caio H. Franco [g, 2], Stefania Ferrari [a], Carolina B. Moraes [g, 2], Anabela Cordeiro-da-Silva [e, h], Glauco Ponterini [a], Joachim Clos [d, **], José María Alunda [b, c, ***], Maria Paola Costi [a, *]

[a] *University of Modena and Reggio Emilia, Via Campi 103, 41125, Modena, Italy*
[b] *Complutense University of Madrid, 28040, Madrid, Spain*
[c] *Instituto de Investigación Hospital 12 de Octubre, Madrid, Spain*
[d] *Bernhard Nocht Institute for Tropical Medicine, D-20359, Hamburg, Germany*
[e] *Instituto de Investigação e Inovação em Saúde, Universidade do Porto and Institute for Molecular and Cell Biology, University of Porto, 4150-180, Porto, Portugal*
[f] *Fraunhofer Institute for Molecular Biology and Applied Ecology Screening Port, Hamburg, Germany*
[g] *Laboratório Nacional de Biociências (LNBio), Centro Nacional de Pesquisaem Energia e Materiais (CNPEM), 13083-100, Campinas, SP, Brazil*
[h] *Departamento de Ciências Biológicas, Faculdade de Farmácia da Universidade do Porto (FFUP), Porto, Portugal*

ARTICLE INFO

Article history:
Received 29 May 2019
Received in revised form
1 August 2019
Accepted 2 September 2019
Available online 5 September 2019

Keywords:
Leishmaniasis
Flavonoid-like scaffold
Pharmacokinetic studies
Drug resistance
Genomic studies
Fluorescence

ABSTRACT

Leishmaniasis, a major health problem worldwide, has a limited arsenal of drugs for its control. The appearance of resistance to first- and second-line anti-leishmanial drugs confirms the need to develop new and less toxic drugs that overcome spontaneous resistance. In the present study, we report the design and synthesis of a novel library of 38 flavonol-like compounds and their evaluation in a panel of assays encompassing parasite killing, pharmacokinetics, genomics and ADME-Toxicity resulting in the progression of a compound in the drug discovery value chain. Compound **19**, 2-(benzo[*b*]thiophen-3-yl)-3-hydroxy-6-methoxy-4*H*-chromen-4-one, exhibited a broad-spectrum activity against *Leishmania* spp. (EC_{50} 1.9 μM for *Leishmania infantum*, 3.4 μM for *L. donovani*, 6.7 μM for *L. major*), *Trypanosoma cruzi* (EC_{50} 7.5 μM) and *T. brucei* (EC_{50} 0.8 μM). Focusing on anti-*Leishmania* activity, compound **19** challenge *in vitro* did not select for resistance markers in *L. donovani*, while a Cos-Seq screening for dominant resistance genes identified a gene locus on chromosome 36 that became ineffective at concentrations beyond EC_{50}. Thus, compound **19** is a promising scaffold to tackle drug resistance in *Leishmania* infection. *In vivo* pharmacokinetic studies indicated that compound **19** has a long half-life (intravenous (IV): 63.2 h; *per os* (PO): 46.9 h) with an acceptable ADME-Toxicity profile. When tested in *Leishmania* infected hamsters, no toxicity and limited efficacy were observed. Low solubility and degradation were investigated spectroscopically as possible causes for the sub-optimal pharmacokinetic properties. Compound **19** resulted a

* Corresponding author. University of Modena and Reggio Emilia, Via Campi 103, 41125, Modena, Italy.
** Corresponding author. Bernhard Nocht Institute for Tropical Medicine, D-20359, Hamburg, Germany.
*** Corresponding author. Complutense University of Madrid, 28040, Madrid, Spain.
E-mail addresses: clos@bni-hamburg.de (J. Clos), jmalunda@ucm.es (J.M. Alunda), mariapaola.costi@unimore.it (M.P. Costi).
[1] C.B. and M.D.J.A. contributed equally and are considered as co-first authors.
[2] Present Address: C.B. Department of Biomedicine, University of Basel, Mattenstrasse 28, 4058 Basel, Switzerland. C.H.F. University of Coimbra 3004-504, Coimbra, Portugal. C.B.M Department of Microbiology, Institute of Biomedical Sciences, University of São Paulo, 05508-900 São Paulo – SP, Brazil.

https://doi.org/10.1016/j.ejmech.2019.111676

specific compound based on the screening against a protein set, following the intrinsic fluorescence changes.

1. Introduction

Leishmania spp. are obligate protozoan parasites of cells of the mononuclear phagocytic system and cause a wide spectrum of diseases, from cutaneous lesions to potentially fatal visceral infections [1]. Leishmaniasis represents a huge burden since an estimated 12 million people are infected with different species of *Leishmania* [2]. Despite the serious health, economic and social consequences, effective vaccines are lacking and the limited arsenal of anti-leishmanial drugs has severe drawbacks including toxicity, poor efficacy and high treatment costs. Five main drugs are in therapeutical use against leishmaniasis, as reported by the World Health Organization. Miltefosine represents the first and only oral drug approved for this disease. Among Neglected Tropical Diseases (NTDs), leishmaniasis is considered to be one of the most challenging infections and its control is hampered by its complex epidemiology and by pathogen resistance [3]. The first line antimony-containing drugs have been in use since the 1920s and face wide-spread drug resistance (DR) in key endemic regions, and even the newer drugs encounter therapy-resistant cases [4,5]. DR is usually due to a decrease in the active drug concentration within the parasite cell that results from increased efflux, reduced uptake or amplified expression of the targeted enzyme. Resistance against classic first-line antimonial therapy has been observed in patients and produced *in vitro* to analyze the main mechanisms involved in this process [6]. A decrease of Sb(III) inside the cell has been observed in several *Leishmania* mutant strains developed in laboratory [7]. Resistance to established second-line therapeutics, such as pentamidine and amphotericin B (AmB) has also been induced *in vitro*. Resistance to AmB has been associated with a variation in cell membrane fluidity, while resistance to pentamidine has been shown to be related to a change in arginine and polyamine concentrations in the cell [8]. The appearance of resistance to established first- and second-line anti-leishmanial drugs stresses the demand to develop novel, less toxic and more effective drugs that would not likely develop spontaneous resistance [9]. To accelerate the discovery of anti-leishmanial drugs, phenotypic approaches offer the potential to identify compounds that are active against the intracellular parasites because they take into account membrane permeability, cell uptake and cell efflux mechanisms. Aiming to use such approaches to select the most promising compounds, suitable counter-screens, including screening against mammalian cells, need to be performed to filter out cytotoxic compounds [10]. This approach has been successfully implemented in NTD drug discovery [11,12]. A wide range of chemical structures, including flavonols (3-hydroxy-2-phenylchromen-4-one), has been investigated in drug discovery programs with the aim of identifying novel anti-leishmanial and anti-trypanosomal agents [13–16]. Recently, we proposed classic hydroxylated and methoxylated flavonols as promising hits against trypanosomatidic infections [16]. However, these compounds displayed only a low potency against *Leishmania* species.

In the search for novel anti-leishmanial compounds, we report herein the design and synthesis of 22 classical flavonols modified with heteroaromatic rings and biphenyl moieties conferring inherent chemical diversity. These structural modifications allowed to explore a novel chemical space around classical flavonols and to secure intellectual property [17]. Despite their well-known multitargeting behavior, flavonoids remain important core structures in the medicinal chemistry field [18]. This compound library was evaluated *in vitro* against *L. infantum* and compound **19** displayed an interesting anti-leishmanial activity. Sixteen additional derivatives (compounds **23**-**38**) were subsequently designed and synthesized to explore the Structure Activity Relationships (SAR) of this series. To assess its spectrum of activity, compound **19** was also screened against *L. donovani*, *L. major*, *T. brucei* and a panel of *T. cruzi* strains. Resistance studies showed that no significantly resistant parasites could be selected from a *L. donovani* population during a 78-day challenge with compound **19** at the EC_{50}/EC_{75}, indicating a low propensity of the parasites to develop resistance against **19**. Pharmacokinetic studies of compound **19** pointed out its long half-life and suitable profile for *in vivo* evaluation in *L. infantum* infected hamsters. In the mice model, we observed a decrease in parasite load in spleen. Compound a low toxicity, while spectroscopic studies showed high lipophilicity and high percentage of plasma binding, securing inhibitor transport in the bloodstream. Compound **19** offers the potential to expand the lead pipeline in anti-leishmanial therapy by tackling the important challenge of drug resistance in the discovery of new drugs for *Leishmania* infections.

2. Chemistry

The design, synthesis and *in vitro* evaluation of natural and synthetic compounds against *T. brucei* and *L. infantum* have shown that methoxylated and hydroxylated classical flavonols are potent anti-*T. brucei* agents (EC_{50} 1–20 μM) and have limited activity against *Leishmania* spp. [16].

Herein, we report that replacement of the phenyl ring of the classical flavonols with heteroaromatic rings and biphenyl moieties leads to a novel anti-leishmanial scaffold. Specifically, we have introduced furan, 3-/4-/5-methylthiophene, pyridine, quinoline, indole, 1-methylindole, benzothiophene and 1,3-benzodioxole rings (Fig. 1 and Table 1).

Compound **19** showed potent anti-leishmanial activity and a SAR study on ring A and on the 3-OH of the chromen-4-one scaffold has been carried out. The chemical structures of the synthesized derivatives of compound **19** are shown in Table 2.

The synthetic procedure for the preparation of these compounds is shown in Scheme 1.

The chalcone intermediates (**39**–**58**) were synthesized by Claisen-Schmidt condensation using substituted acetophenones and benzaldehydes in the presence of NaOH as the base. The reaction was carried out in ethanol as previously reported [16]. For the synthesis of compound **20**, piperidine was used instead of a strong base. In some cases, the chalcones were not isolated as pure products and were used for the following step without further purification (see the Experimental Part for details). The chalcones were converted into the corresponding flavonol-like compounds (**1**, **2**, **5**, **6**, **8**, **9**, **11**, **13**, **17**–**20** and **22**–**32**) using the Flynn-Algar-Oyamada method for epoxidation and subsequent intramolecular cyclization of the open-chain structure [19]. The reaction was performed with hydrogen peroxide in aqueous base (1 M NaOH). The hydroxylated flavonols (**3**, **4**, **7**, **10**, **12** and **21**) were synthesized by

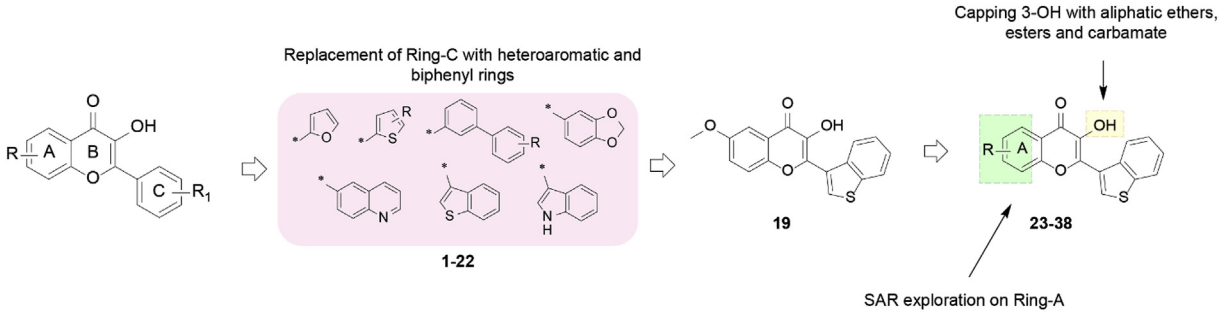

Fig. 1. Structure-Activity Relationship (SAR) studies.

Table 1
Structure of the synthesized flavonol-like compounds bearing heteroaromatic and biphenyl rings. Compounds **2**, **3**, **13**, **17**, **20** and **22** have been previously described in the literature, while compounds **1**, **4**–**12**, **14**-**16**, **18**, **19** and **21** are novel structures and have not been previously reported.

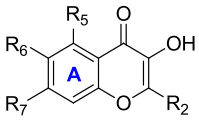

Comp.	R_2	R_5	R_6	R_7	Comp.	R_2	R_5	R_6	R_7
1		H	OCH_3	H	**12**		H	H	OH
2		H	H	OCH_3	**13**		H	CH_3	H
3		H	OH	H	**14**		H	OCH_3	H
4		H	H	OH	**15**		H	OH	H
5		H	OCH_3	H	**16**		H	OCH_3	H
6		H	H	OCH_3	**17**		H	H	OCH_3
7		H	OH	H	**18**		H	OCH_3	H
8		H	CH_3	H	**19**		H	OCH_3	H
9		OCH_3	H	H	**20**		H	OCH_3	H
10		OH	H	H	**21**		H	OH	H
11		H	H	OCH_3	**22**		H	OCH_3	H

cleavage of the methoxy protecting groups using boron tribromide (Scheme 1).

The procedure for the synthesis of compounds **14**–**16** is shown in Scheme S1 of the Supporting Information. The first step involved a Suzuki cross-coupling reaction of alkyl boronic acid with 3-bromobenzaldehyde. The synthesized aldehydes (**59** and **60**) reacted with 2′-hydroxy-5′-methoxyacetophenone in the presence of NaOH. The chalcones were not isolated as pure products but were directly converted into the corresponding flavonols using the procedure described above.

Compound **19** was synthesized as reported in Scheme 1 and subsequently converted into the corresponding esters (**33**–**35**), ethers (**37** and **38**) and carbamates (**36**). For the synthesis of esters and carbamates, compound **19** was treated with an excess of acyl

Table 2
Chemical structure of the novel derivatives of compound **19** (compounds **23**–**38**).

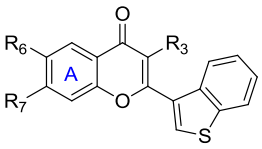

Comp.	R_3	R_6	R_7	Comp.	R_3	R_6	R_7
23	OH	CH_3	H	**31**	OH	H	Cl
24	OH	Br	H	**32**	OH	H	OCH_2CH_3
25	OH	F	H	**33**		OCH_3	H
26	OH	Cl	H	**34**		OCH_3	H
27	OH	H	H	**35**	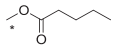	OCH_3	H
28	OH	H	OCH_3	**36**		OCH_3	H
29	OH	H	CH_3	**37**		OCH_3	H
30	OH	H	F	**38**		OCH_3	H

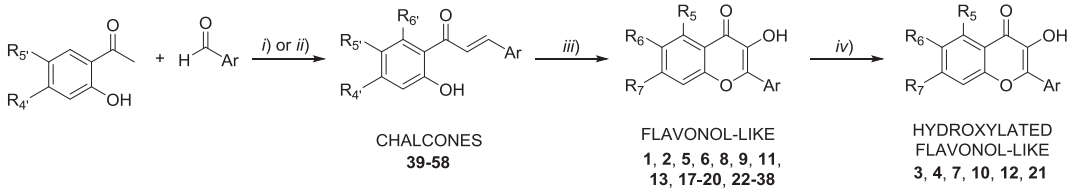

Scheme 1. Reagents and conditions: (i) NaOH (3 M), EtOH, r.t.; (ii) Piperidine, EtOH, reflux; (iii) H_2O_2, NaOH (1 M), EtOH, r.t.; (iv) BBr_3 (1 M in dry DCM), dry DMC, 0 °C, r.t. With the exception of compound **46**, all chalcones were synthesized following procedure (i).

chloride in dry dichloromethane (DCM) in the presence of triethylamine. For the synthesis of ethers, an alkyl halide was added to a solution of compound **19** in dry DMF and in the presence of K_2CO_3 (Scheme S2 of the Supporting Information).

3. Results

3.1. *In vitro* evaluation against T. brucei and L. infantum

With the exception of compound **22**, the novel library of flavonol-like compounds (**1**–**21**) was evaluated against *L. infantum* intracellular amastigotes and *T. brucei* bloodstream forms. For compounds causing a >70% reduction of parasite loads or a >70% parasite growth inhibition at 10 μM, dose-response experiments were performed to determine their potencies. In addition, the compound series was assessed for cytotoxicity in THP1 macrophage-like cells to estimate the half maximal cytotoxicity concentration (CC_{50}) and the selectivity index (SI = CC_{50}/EC_{50} parasite). Most of the synthesized compounds displayed low micromolar potency against *T. brucei* (Table S1 of the Supporting Information). All compounds bearing a furan (**1**–**4**) and compound **18** bearing a quinoline were not active towards *T. brucei* in the concentration range evaluated (from 78 nM to 10 μM). Compounds bearing a methylated thiophene showed activity only when a methoxy group (**5**, **6**, **9** and **11**) or a methyl group (**8** and **13**) was linked to ring A of the chromen-4-one scaffold (EC_{50} < 6 μM). In fact, compounds with a methyl-thiophene and a hydroxyl group linked to ring A (**10** and **12**) did not inhibit *T. brucei* cell growth, with the exception of **7** (EC_{50} = 4.9 μM). The SI of compounds with a methyl thiophene were <10 with the exception of compound **8** which showed a SI of 36. Compounds **14**–**16**, bearing a biphenyl ring, had low micromolar potency against *T. brucei* with EC_{50} values of 3.0, 1.7, 3.9 μM, respectively. Compound **15**, which contains hydroxyl groups linked to the biphenyl ring, was the most potent and selective biphenyl derivative (SI = 15). Compound **19**, possessing a benzothiophene ring, was more active and selective than the corresponding methyl-thiophene derivative **5** (EC_{50} = 0.8 and 5.7 μM, SI = 33 and 4, respectively). Replacement of the sulfur of compound **19** with a nitrogen (**20**) yielded a decrease in activity and a significant decrease in SI (EC_{50} = 0.8 and 1.4 μM, SI = 33 and 8, respectively). Compound **17**, bearing a 1,3-benzodioxole, was the most active and selective molecule towards *T. brucei* (EC_{50} = 0.4 μM, SI = 250). The most promising compounds are depicted in Fig. 2A. Very recently, we have validated compound **17** as an anti-*T. brucei* agent and have carried out SAR studies and discovered follow-up hits [20]. Herein, we focus our attention on the identification of flavonol-like compounds with a broad spectrum of activity, able to inhibit *Leishmania* parasites. Therefore, the library of 22 compounds was evaluated for the anti-parasitic activity against *L. infantum*-infected macrophages. Compound **19** showed an EC_{50} for *L. infantum* comparable to that of miltefosine, the drug of choice to treat *Leishmania* infections when resistance to antimonials is

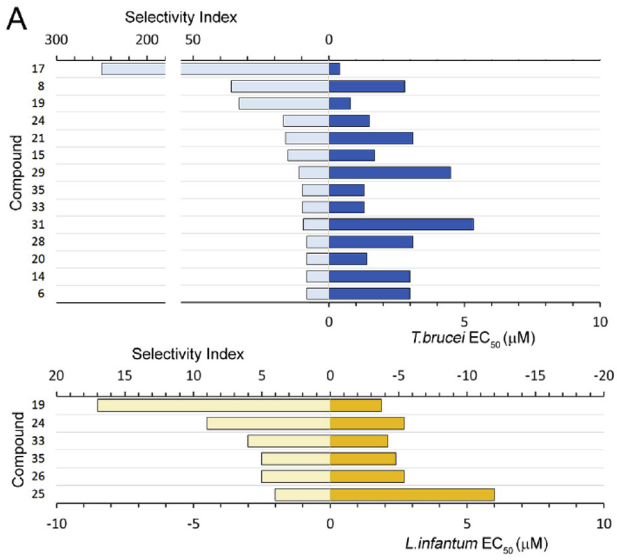

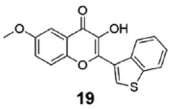

B

19

T. brucei

Entry	*T. brucei* EC_{50} (μM)
19	0.8
PEN	0.016

***Leishmania* spp.**

Entry	*L. infantum* EC_{50} (μM)	*L. donovani* EC_{50} (μM)	*L. major* EC_{50} (μM)
19	1.88	3.4	6.7
MIL	2.51	9.0	-

***T. cruzi* strains**

Entry	Y strain infected HG39 cells EC_{50} (μM)	Silvio X10/1 EC_{50} (μM)	Y EC_{50} (μM)	ARMA13 cl11 EC_{50} (μM)	92.80 cl2 EC_{50} (μM)	CL Brener EC_{50} (μM)
19	7.5	0.3 ± 0.09	0.9 ± 0.34	1.2 ± 0.01	0.7 ± 0.06	0.6 ± 0.33
MIL	12.5	-	-	-	-	-
BEN	2.4	3.9 ± 0.98	2.2 ± 1.81	5.1 ± 3.11	0.6 ± 0.05	1.0 ± 0.31

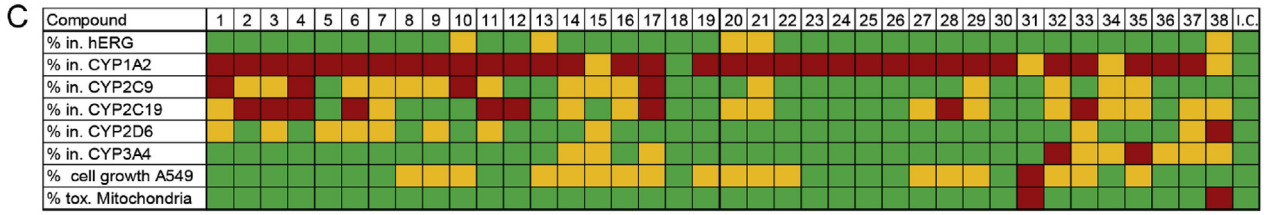

Fig. 2. **(A)** Selectivity index and EC_{50} of compounds showing activity towards *T. brucei* (upper panel) and *L. infantum* (bottom panel). The selectivity index is reported on the left (light color bars), while EC_{50} is reported on the right (dark color bars). **(B)** Inhibitory profile of compound **19** against *T. brucei*, *Leishmania* spp. and *T cruzi* strains. **(C)** Early toxicological data of compounds **1**-**38**. All the assays were performed at 10 μM and the data ranges are reported using a traffic light system. An ideal compound (I.C.) possesses all the parameters in green. The cells are colored in green when the percentage inhibition of CYP isoforms, *h*ERG, Aurora B kinase and mitochondrial toxicity is 0–30%. Cells are colored in red when data indicate toxicity (percentage of inhibition of CYP isoforms, *h*ERG, Aurora B kinase and mitochondrial toxicity ≥60). Yellow color indicates inhibition values between 30 and 60% for slightly toxic compounds. Compounds are considered as non-cytotoxic (green) for A549 cell line when growth is 60–100%, cytostatic (yellow) when 0–59% and cytotoxic (red) when <0. (For interpretation of the references to color in this figure legend, the reader is referred to the Web version of this article.)

observed, and a higher SI (EC_{50} for **19** = 1.88 ± 0.32 μM, SI = 17; EC_{50} for miltefosine = 2.6 ± 0.4 μM, SI = 5). Therefore, compound **19** was screened against different *Leishmania* species and *T. cruzi* to determine its spectrum of anti-parasitic activity.

3.2. Evaluation of compound *19* towards L. major, L. donovani and T. cruzi

Compound **19** showed EC_{50} in the low micromolar range also against *L. donovani* (EC_{50} = 3.4 μM) and *L. major* promastigotes (EC_{50} = 6.7 μM). Thus, it represents a promising compound for both visceral (VL) and cutaneous leishmaniasis (CL). Moreover, compound **19** was active against the *T. cruzi* infection of human glioblastoma cells (HG39), with an EC_{50} of 7.5 μM, compared with an EC_{50} of 12.5 μM for miltefosine (Fig. 2B). It was screened against the intracellular amastigotes of a panel of *T. cruzi* strains: Silvio X10/1 (TcI), Y (TcII), ARMA13 cl1 (TcIII), 92.80 cl2 (TcV) and CL Brener (TcVI), and was found to be active against all five strains. The potency of compound **19** was superior to the reference compound benznidazole in all tested strains, except for strain 92.80 cl2 where the EC_{50} values of both compounds were similar (Table 3).

3.3. Structure-Activity Relationship (SAR) studies around compound *19*

Considering the anti-parasitic activity and selectivity of compound **19**, SAR studies were carried out for hit confirmation. Sixteen derivatives of compound **19** (**23**–**38**) were designed, synthesized and biologically evaluated towards *T. brucei* and *L. infantum* parasites (for chemical structures, see Table 2). With the exception of five compounds (**30**, **32**, **36**–**38**), all molecules had significant activity against *T. brucei* (EC_{50} < 6 μM), whilst only compounds **24**-**26**, **33** and **35** showed activity towards *L. infantum* (EC_{50} < 6 μM) (Table S2 of Supporting Information). When the OCH_3 in position 6 of compound **19** was replaced with CH_3, Br, F and Cl (compounds **23**, **24**, **25** and **26**, respectively) anti-*T. brucei* activity was maintained (EC_{50} < 2 μM), and compounds **24**-**26**, bearing halogens in position 6, showed anti-*Leishmania* activity with EC_{50} < 6 μM. Compounds bearing an unsubstituted ring A (**27**), a methoxy group or a methyl group in position 7 (**28** and **29**) showed anti-trypanosomal activity (EC_{50} = 2.6, 3.1 and 4.5 μM, respectively), but were not active against *L. infantum*. The presence of an ester instead of a hydroxyl group in position 3 led to activity towards

Table 3
Potency of compound **19** and the reference compound benznidazole against a panel of *T. cruzi* strains.

***T. cruzi* strains**	**Silvio X10/1**	**Y**	**ARMA13 cl1**	**92.80 cl2**	**CL Brener**
EC_{50} (μM) comp. 19	0.3 ± 0.09	0.9 ± 0.34	1.2 ± 0.01	0.7 ± 0.06	0.6 ± 0.33
EC_{50} (μM) benznidazole	3.9 ± 0.98	2.2 ± 1.81	5.1 ± 3.11	0.6 ± 0.05	1.0 ± 0.31

Data represent mean ± standard deviation of two independent experiments.

both *T. brucei* and *L. infantum* (compounds **33** and **35**) ($EC_{50} < 4\ \mu M$), while compounds **36** and **37**–**38**, bearing a carbamate or an ether, respectively, did not possess significant anti-parasitic activity. These results suggest that the free hydroxyl group in position 3 is required for significant compound potency. As for the derivatives of compound **19**, the activity of esters can be related to enhanced hydrolysis with respect to the ethers and carbamates and therefore **19** remains the most promising anti-leishmanial agent. The most potent and selective compounds on *T. brucei* and *L. infantum* are depicted in Fig. 2A, while a summary of the broad spectrum of activity of compound **19** is shown in Fig. 2B. Miltefosine, pentamidine and benznidazole were selected as reference compounds for comparison (Fig. 2B).

3.4. Early ADME-Toxicity profile

The ADME-Toxicity profile of the library of 38 compounds was assessed at 10 μM in a panel of assays comprising *h*ERG, Aurora B kinase, cytochromes (CYP1A2, CYP2C9, CYP2C19, CYP2D6 and CYP3A4), cytotoxicity (A549 cell line) and mitochondrial toxicity. The data are reported in Fig. 2C using a traffic light system to indicate value ranges and in Table S3 of the Supporting Information. With the exception of compounds **10**, **13**, **20**, **21** and **38**, none exhibited toxicity towards *h*ERG, which is a pivotal parameter for proceeding a compound further in the drug discovery process. Overall, the compounds yielded significant inhibition of cytochrome CYP1A2. Some compounds were cytostatic, but only **31** was cytotoxic (cell growth A549 < 0%). With the exception of compounds **31** and **38**, no compound presented mitochondrial toxicity. For compound **19**, EC_{50} towards *L. infantum* was 1.9 μM (SI = 33); the *h*ERG IC_{50} (>100 μM) was over 50-fold greater than the EC_{50} towards the parasite. With the exception of the CYP1A2 IC_{50} (0.4 μM), the IC_{50} against the cytochrome isoforms were >10 μM (IC_{50}: CYP2C9 >100 μM; CYP2C19 > 100 μM; CYP2D6 = 14.8 μM; CYP3A4 >100 μM), thus consistent with the parameters for compound selection and prioritization as reported previously in a similar compound series [16]. The compound slowed the growth of W1-38 cells, but it was not cytotoxic (Fig. 2C).

All compounds were also screened using the FAFdrugs4 software (http://fafdrugs4.mti.univ-paris-diderot.fr, Table S9 of the Supporting Information), a software dedicated to evaluate the potential liabilities as PAINS (pan assay interference compounds) [21]. Considering the above described comprehensive panel of assays used for compounds screening, the flavonol-like scaffold overcomes some of the liabilities typical of classical flavonols such as CYP450 enzymes inhibition and hepatocytes inhibition effects [22]. This suggested that the chemical modifications introduced do not induce the PAINS features in the scaffold. Therefore, compound **19** was selected for further characterization.

3.5. Drug resistance investigation in L. donovani

First, we tested whether compound **19** was effective against antimony-resistant *Leishmania* parasites. Two field isolates of *L. donovani* from Nepal, BPK091 and BPK190 [23] that were respectively inherently sensitive and resistant to antimony treatment, were used to infect mouse bone marrow-derived macrophages. Infected cells were subsequently treated with increasing concentrations of compound **19** (Fig. 3A). Compound **19** is active against both strains, showing 36% and 78% parasite load reduction at 5 μM, against BPK091 and BPK190, respectively, and 69% reduction for both strains at 10 μM, indicating its capacity to eliminate antimony-resistant *L. donovani* from infected macrophages.

Afterwards, we investigated whether spontaneous resistance may overcome compound **19** activities. *L. donovani* promastigotes were grown *in vitro* at the IC_{50} of compound **19** and miltefosine, with DMSO as a negative control. Parasites were seeded (1×10^5/mL) into a medium containing the drugs and grown for 3 days under selective pressure, then seeded again (1×10^5 cells/mL) into a fresh medium containing the respective compounds. Three-day *in vitro* passages were repeated 11 times (>50 generations). Miltefosine-selected cultures showed increasing growth rates after this selection, indicating the development/selection of resistant parasites in the populations. By contrast, growth in the presence of compound **19** remained at <50% throughout the 33 days of selection (Fig. 3B), excluding a spontaneous development of resistance.

With the caveat that the experiments were performed with promastigotes in culture and not with the relevant, intracellular amastigote stage, we conclude that exposure to compound **19** at sub-effective concentrations do not lead to spontaneous resistance. This indicates the absence of compound **19-**tolerant *L. donovani* clones within a population that harbors miltefosine-resistant individual promastigotes.

Reversible gene amplification occurs frequently in *Leishmania* spp. and contributes to the appearance of drug resistance *in vitro* and in the field [25,26]. This includes chromosome ploidy changes, gene copy number variations, but also the extrachromosomal amplification of genomic regions in the form of episomes. The latter mechanism may be mimicked by a cosmid library screening or functional cloning of dominant resistance genes [27]. This approach was recently refined by a combination with next generation sequencing (NGS), called Cos-Seq [28,29]. This strategy (Fig. 3C) was used to identify possible gene markers of compound **19** resistances *in vitro*. Fig. 3C shows the selection process and the isolation of cosmids for NGS.

A *L. donovani* population, randomly transfected with a genomic DNA cosmid library of *L. donovani*, was challenged with miltefosine or compound **19** at EC_{50} using the same, periodic 3-day *in vitro* passage intervals as above. Another population was passaged identically using the solvent DMSO as control. Indeed, by day 37 of the selection, parasites were showing >50% growth compared to the DMSO control, both under miltefosine and under compound **19** challenge (Fig. 3D).

Cosmid DNA from populations selected at IC_{50} for miltefosine and compound **19**, and control cultures were recovered and analyzed by Illumina NGS. Sequence reads (https://www.ncbi.nlm.nih.gov/Traces/study/?acc=PRJNA512372) were aligned to the *L. infantum* genome database using Bowtie2 alignment. One major and one minor alignment peak were recorded (Fig. S1 of the Supporting Information), identifying gene regions on chromosome 36 (position 2,561,981 - 2,592,497) and chromosome 24 (position 357,326–392,031) as possible markers of compound **19** tolerance (Table S4 and Fig. S1 of the Supporting Information).

The selected populations were subjected to further challenge with miltefosine or compound **19** at their respective IC_{75} for another 38 days (25 passages in total). At IC_{75}, miltefosine-selected parasites yielded >75% growth relative to DMSO controls. In contrast, compound **19**-preselected parasites showed no ability to proliferate at the IC_{75} of the compound (Fig. 3D). This indicates that none of the cosmid-based transgenes in the recombinant population (Table S4 of the Supporting Information) is a dominant resistance gene marker for compound **19**, further supporting the notion that compound **19** is comparatively impervious to spontaneous or gene amplification-mediated resistance in *Leishmania*.

3.6. Half-life determination in vivo

Compound **19** bioavailability and half-life were evaluated in BALB/c mice treated IV with 1 mg/kg and PO with 20 mg/kg. Compound **19** was characterized by a long half-life (IV):63.2 h;

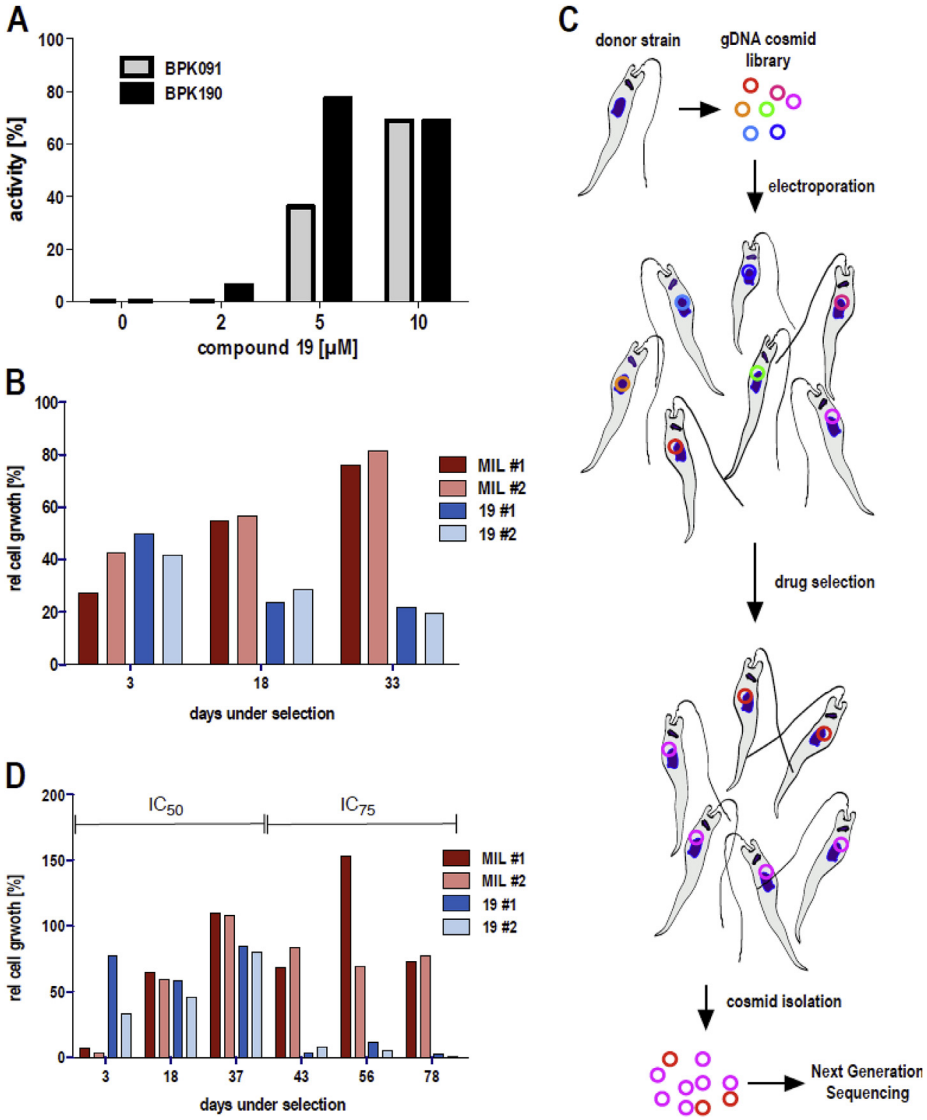

Fig. 3. **(A)** Activity of compound **19** against two strains of *L. donovani*, BPK091 (Sb sensitive, gray) and BPK190 (Sb resistant, black) [23]. Mouse bone marrow-derived macrophages were infected with stationary growth phase promastigotes at Multiplicity Of Infection (MOI) = 10:1. At 24 h p.i., compound **19** was added at 0–10 µM. At 72 h p.i., the infected cells were harvested, total DNA was isolated, and parasite load was determined by qPCR [24]. Activity [%] was defined as reduction of relative parasite load compared to the solvent controls. Bars show the mean of 2 biological replicates. **(B)** Selection for resistance. *L. donovani* strain 1SR promastigotes were seeded at 1×10^5 cells/mL and grown for 3 days at EC_{50} of miltefosine or compound **19** with DMSO solvent controls and in biological duplicates. Cell densities were recorded, and cells were diluted to 1×10^5 cells/mL in drug-containing medium. The selection cycles were repeated 10 times for a total of 33 days. Cell growth relative to DMSO controls is given in [%] at days 3, 18 and 33 of selection. Bars show the mean with SD of 2 technical repeats, from 2 biological samples (#1 and #2) **(C)** Schematic representation of the functional cloning strategy, with pink and red circles symbolizing selected cosmids. **(D)** Cosmid library selection. *L. donovani* strain BPK91 transfected with a genomic DNA cosmid library of strain BPK190 was selected essentially as described in (**A**). After 40 days, the selective pressures of miltefosine and compound **19** were increased to EC_{75}. Cell growth relative to DMSO controls (% inhibition) at days 3, 18, 37 (EC_{50}) and 43, 56, 78 (EC_{75}) of selection. Bars show the mean with SD of 2 technical repeats, from 2 biological samples (#1 and #2). (For interpretation of the references to color in this figure legend, the reader is referred to the Web version of this article.)

(PO): 46.9 h and a C_{max} higher than the EC_{50} towards *L. infantum* (*ca.* 1.9 µM) (Table 4).

3.7. Clinical course of the infection and toxicity of compound **19** in hamsters

Efficacy studies were performed in hamster as it is considered to be the best rodent model for human VL [30] on the basis of progression of the disease including organs affected, lesions and final outcome [31]. Cyclodextrins (CDs) have been shown to enhance permeability and increase activity of several anti-leishmanial drugs [32,33]. Compound **19**, formulated with or without CDs and administered PO (40 mg/kg/day; 20 mg/kg/every 12 h) for 10 days, was tested on Syrian hamsters that had been infected with *L. infantum* for 15 weeks. Infection with *L. infantum* did not cause significant changes of food uptake and behavior, or clinical signs in the test animals. Lesions were absent or mild and included conjunctivitis, periorbital and abdominal alopecia. Animals showed comparable live weight gain ($P > 0.05$) irrespective of their infection status (Fig. S2 of the Supporting information).

Treatment with compound **19**, free (8% v/v DMSO) or formulated with CDs (30% or 50%), did not elicit any noticeable adverse effect along treatment days. In contrast, treatment-using miltefosine (20 mg/kg/day, 10 days) provoked some adverse effects in 6 out of 8 animals from the group, including distress, itching, dizziness and nausea (Fig. 4A). These effects were transient and disappeared once

Table 4
Pharmacokinetic parameters of compound **19**.

Compound	Dose (mg/kg) and route	C_{max} (ng/mL)	C_{max} (μM)	T_{max} (h)	AUC_{tot} (ng/mL h)	AUC_{tot} (nmol/mL h)	Half life (h)
19	1 (IV)	1,540	4.76	0.08	5,280	16.28	63.2
19	20 (PO)	630	1.96	1.00	12,500	38.54	46.9

the drug administration was completed. Plasma creatinine and urea values were homogeneous within and among hamster groups. In contrast, transaminases (ALT and AST), particularly AST, showed intergroup and intragroup variations and some outliers. Although most of the values were within the expected physiological range significant differences ($P < 0.01$) were found in alkaline phosphatase levels, with the highest value being found in CDs 50% treated hamsters. However, this difference lacks significance since animals treated with CDs 50% plus compound **19** did not show any difference (Fig. S3 of the Supporting Information). Under necropsy, no evident gross pathology lesions were observed in liver and spleen of most animals. Only 3 out of 47 infected animals showed apparent congestive hepatopathy, although no spleen or liver enlargement was found (Table S5 of the Supporting Information).

The ability of **19** to evade resistance mechanisms upon drug challenge in Leishmania parasites, its efficacy against Sb resistant strains, its low toxicity and the preliminary PK data reported, suggest the suitability for in vivo efficacy studies in hamsters.

3.8. Serum antibody response against *L. infantum* in hamsters

Serum antibody response against *Leishmania* can give information on the spread of infection and thus it is a convenient tool to follow up infection and recovery in experimental infections in hamsters [34,35]. The serum anti-*Leishmania* IgG response, determined by ELISA, confirmed the efficacy of the inoculation since all infected groups displayed a steady increase of specific IgG. Untreated hamsters (only receiving DMSO or CDs) raised their antibody levels, whereas animals treated with compound **19** or miltefosine showed, after medication, equal or lower antibody mean levels at the end-point of the experiment (14 weeks *vs* 18 weeks sampling, Fig. 4B). Wide intra-group variations among animals precluded the observation of significant differences, with the exception for miltefosine ($P < 0.05$). Due to the close correlation between leishmanial infection and specific antibody response, these findings provided indirect evidence of the anti-leishmanial activity of compound **19**. Moreover, the higher antibody levels in untreated animals suggested that the reduction in treated hamsters was not due to the vehicle (DMSO or CDs).

3.9. Anti-leishmanial efficacy of compound ***19***

Parasite burden (PB) was determined using Leishman-Donovan units (LDU) by counting the amastigotes found in 500 cells in spleen and liver (Table S6 of the Supporting information). None of the uninfected control animals had *L. infantum* amastigotes at the time point of euthanasia. Hamsters receiving the vehicle (8% v/v DMSO) were infected in both liver and spleen (liver: $5.3 \pm 3.0 \times 10^6$ amastigotes/g; spleen: $9.1 \pm 2.6 \times 10^6$ amastigotes/g). As expected there was a general correlation between liver and spleen infection, with higher PB in spleen. These findings confirm the spleen as the main target for *L. infantum* in hamster and its value as surrogate model for human infections [30]. Miltefosine elicited a strong reduction of PB compared to the untreated infected controls in liver ($81.2 \pm 28.3\%$ reduction) and, particularly, in spleen ($97.33 \pm 3.9\%$ reduction, Fig. 4C) and four hamsters apparently cleared the leishmanial infection after miltefosine treatment (#59, #14, #74, #29). A wide intragroup variation was observed in animals infected and treated with compound **19** + CDX. The average PB in the spleen

A

Group	Animal Id	Day 1	Day 2	Day 3	Day 4	Day 5	Day 6	Day 7	Day 8 - 10	Observations
Miltefosine 20mg/kg/day (n=8)	51			+	++	++	+			Nausea, dizziness, distress
	23									
	59									
	1		+		+					Itching, distress
	14				+	++		+		Nausea, dizziness, distress
	65						+			Nausea, distress
	74		+					+		Distress, dizziness
	29		+	++	+	++		+		Nausea, dizziness, distress

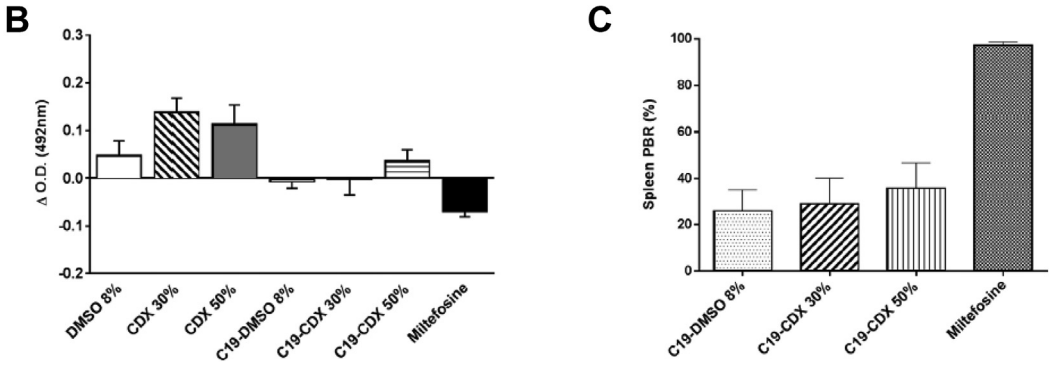

Fig. 4. (A) Score of immediate adverse effects observed after administration of miltefosine (20 mg/kg/day) to hamsters with *Leishmania infantum* infection undergoing ten days of treatment. (+): no adverse effects; (++): mild effects; (+++): significant effects. **(B)** Variation (mean ± standard error of the mean) of serum anti-*Leishmania* IgG levels (Optical density values of pretreatment sampling − Optical density post treatment) in hamsters infected with *L. infantum* and treated with vehicles or vehicles + compound **19**, determined by ELISA. **(C)** Reduction (%) of *Leishmania* burden in spleen of infected and treated hamsters. Values are mean ± standard error of the mean.

of hamsters treated with compound **19** + 50% CDs was lower (35.8 ± 28.7% reduction) than that observed in the hamsters treated with free compound **19** (25.9 ± 24.4% reduction) or with 30% CDs (28.8 ± 30.1% reduction) although differences were not significant due to the intragroup variations. These results indicate that a limited leishmanicidal/leishmaniostatic activity of compound **19** can be observed, together with a modest effect of the CDs formulations on compound efficacy.

3.10. Plasma concentration in treated hamsters and lipophilicity of compound *19*

We investigated if the changes in blood levels of compound **19** could be related to the observed low *in vivo* efficacy. To this aim, we determined the plasma levels of compound **19** and miltefosine in infected and treated hamsters 72 h after the final treatment (Table S7 of the Supporting information). The results obtained in the miltefosine-treated group (59.3 ± 13.7 μM) were in agreement with the long half-life of the molecule and the anti-leishmanial efficacy achieved with the therapeutic regimen employed. On the other hand, all the groups treated with compound **19** had plasma concentrations of the drug lower than the estimated EC_{50} value for *L. infantum* (1.88 ± 0.32 μM) irrespective of the vehicle used (DMSO 8%: 0.044 ± 0.024 μM; 30% CDs: 0.076 ± 0.125 μM; 50% CDs: 0.038 ± 0.026 μM). For ethical reasons, no repeated blood samplings during treatment were performed. However, the results suggest that the low efficacy of compound **19** in hamsters infected with *Leishmania* is likely due to its low blood level, possibly related to a too high lipophilicity and a poor intestinal absorption.

We tackled the problem of the low plasma concentration of compound **19** in hamsters by investigating whether it might be due to high lipophilicity and/or chemical instability. The UV−vis absorption spectrum at 60 μM solution of compound **19** in DMSO, kept at room temperature in the dark, was reproduced within 1% one day after solution preparation. In contrast, a relatively rapid decrease in the absorption was consistently observed in a solution of compound **19** in PBS (pH 7 and pH 8), with no obvious effect of the exposure to daylight. For a 60 μM solution, a 80% decrease in the maximum absorbance was observed at 25 °C in 50 min (Fig. S4 of the Supporting Information), and 20 min after solution preparation, the absorbance was reduced by 50%. To test the hypothesis that a water-assisted oxidation of compound **19** was responsible for its disappearance, nitrogen was bubbled through the solution immediately after preparation for 2 min to replace the dissolved oxygen and prevent oxidation. During this process, an immediate fading of the solution was observed resulting in >90% reduction in the absorbance. The experiment was repeated by replacing nitrogen with air, and the same result was obtained. These observations are consistent with segregation of a large fraction of compound **19** from the water bulk, where it is spectrophotometrically observable, to the water/air(nitrogen) interface, where it is no more accessible to the spectrophotometer beam, a migration mechanically accelerated by gas bubbling. To support the view that the disappearance of compound **19** from aqueous solutions is due to segregation of the compound from bulk water, rather than to chemical instability, we observed a large recovery of absorption by adding 20 μM human serum albumin to the nitrogen- or air-bubbled solutions of the compound (Fig. S5 of the Supporting Information). Albumin offers a suitable environment to this compound and, at least partially, resolubilizes it. Thus, the low levels of compound **19** found in plasma may result from its lipophilicity and the related tendency to escape bulk water. Albumin can bind **19** and transport it through the bloodstream.

3.11. Binding of compound *19* to proteins revealed by its fluorescence

To set the basis for an understanding of the off-targets binding profile of compound **19**, in addition to the early-tox profile (section 3.4), we evaluated its ability to bind to a set of proteins taking advantage from the enviromental dependence of its fluorescence properties [36]. This, and the resulting possibility to discriminate between the free and protein-bound states of **19** in cellular environments, offer a valuable observable, alternative to the use of tags, for fluorescence-based investigations of the binding of compound **19** with both catalytic and non-catalytic soluble proteins, to be performed in subsequent stages of the drug discovery path (e.g., target and off-target engagement in cells). We described the changes in fluorescence properties of this compound due to its interaction with five proteins. When human or bovine serum albumin (HSA and BSA) were added to a freshly prepared solution of compound **19**, changes in the steady-state emission spectrum and anisotropy and in the lifetime profile were observed (Fig. 5A–D). While the intensity of the free-compound emission at 450 nm decreased, a new band with a maximum at 530–535 nm appeared whose intensity correlated with albumin concentration (see Figs. S6 and S7 of the Supporting Information for the case of HSA). At [**19**] = 5 μM, the emission intensity at 450 nm was halved at an albumin concentration of 0.6 ± 0.1 μM. The 530 nm emission band, characteristic of a stable **19**/protein complex, increased and was saturated at higher albumin concentrations, half of the saturating intensity being reached at [HSA] = 2 μM and [BSA] = 12 μM. These figures roughly corresponded to the dissociation constants of compound **19** versus the two proteins and confirmed their ability to keep it solubilized. The emission time decay of compound **19** in aqueous buffer was a single exponential (90–95% abundance) with a very short lifetime, 0.32 ± 0.05 ns (red in Fig. 5D). The decays of the **19**/protein complexes exhibited profiles with a new prominent component with lifetimes of 5.1 ± 0.05 ns (60% abundance, HSA) and 5.5 ± 0.07 ns (50% abundance, BSA) (Fig. 5D). Also, as a clear result of a decrease in the rotational mobility of the fluorophore due to its binding to BSA and HSA, the emission anisotropy increased from 0.06 for the free-molecule to 0.21 ± 0.02 and 0.185 ± 0.02, respectively. Addition of three other proteins, pepsin, trypsin and casein, to compound **19** also increased emission in the 530 nm region (Fig. 5C) and the abundance of the 5.5 ± 0.07 ns lifetime component (black and green in Fig. 5D). However, at fixed protein concentration (10 μM in Fig. 5C), these proteins showed weaker effects than the two albumins, likely resulting from lower affinities for compound **19**.

In conclusion, among the five proteins assayed, only HSA showed a K_d below 10 μM and is therefore of high biological significance for specific *versus* non-specific binding (the latter corresponding to K_ds higher than 12 μM [36]).

4. Discussion

Treatment and control of leishmaniasis relies on a small number of available anti-parasitic drugs, most of which are compromised by a limited activity spectrum, severe side effects and emerging drug resistance [37–39]. This highlights the need for novel and more effective drugs with a low risk of resistance. Herein, we report the design, synthesis and biological evaluation of a novel library of 38 flavonol-like compounds. Compound **19**, bearing a benzothiophene, was associated with an *in vitro* anti-parasitic activity against *L. infantum* comparable to that of miltefosine (EC_{50} = 1.88 ± 0.32 μM; EC_{50} miltefosine = 2.65 ± 0.4 μM) and an improved SI (**19** SI = 17, miltefosine SI = 5). Compound **19** was screened against *L. major* and *L. donovani* and was shown to be

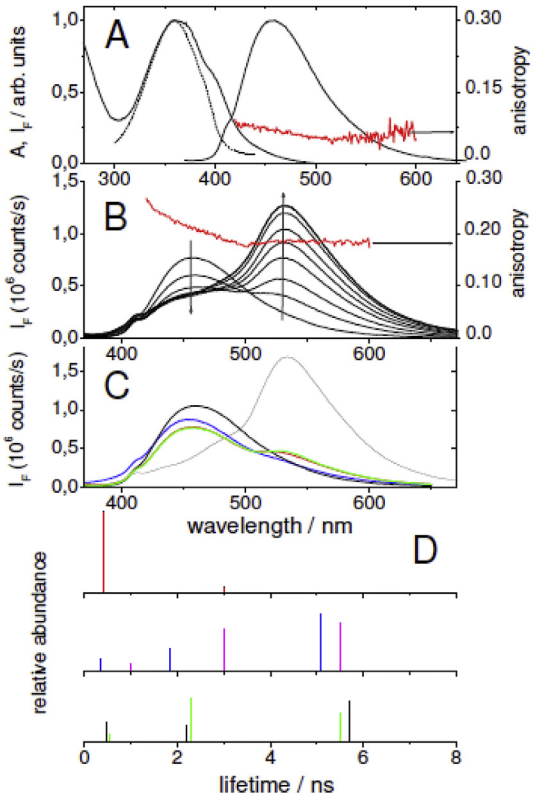

Fig. 5. Fluorescence properties of compound **19** in aqueous solution at pH 8: **(A)** absorption, emission, excitation (dashed, $\lambda_{em} = 450$ nm) and emission anisotropy (red) spectra; **(B)** emission spectra of 5 μM **19** with 0, 0.5, 1, 2, 3, 4, 5, 7 and 10 μM HSA and emission anisotropy (red) of the final solution; **(C)** emission spectra of 5 μM **19** alone (black curve with maximum at 455 nm) and with 10 μM BSA (black curve with maximum at 533 nm), pepsin (blue), trypsin (green) and casein (red); **(D)** lifetime distributions measured at the emission wavelengths of 450 nm for **19** alone (red), and 530 nm for 5 μM **19** with 10 μM HSA (blue) and BSA (magenta), with 130 μM pepsin (black) and with 80 μM casein (green). The relative abundance of a component with a given lifetime represents the fraction of all emitted photons corresponding to that component; the 0.4 ns component in red ha a relative abundance of 0.93. For all steady-state emission and anisotropy measurements, $\lambda_{exc} = 360$ nm; for the time-resolved measurements, $\lambda_{exc} = 340$ nm. (For interpretation of the references to color in this figure legend, the reader is referred to the Web version of this article.)

more potent than miltefosine towards both *L. donovani* (EC_{50} **19** = 4.6 μM, miltefosine = 10.8 μM) and *L. major* (% efficacy at 5 μM: compound **19** = 60%, miltefosine = 20%, EC_{50} compound **19** = 5 μM). Compound **19** was active also towards *T. brucei* (EC_{50} = 0.8 μM; EC_{50} pentamidine = 1.5 nM) and, in a panel of *T. cruzi* strains (Silvio X10/1, Y, ARMA cl1, 92.80 cl 2, CL Brener), it showed potency comparable to that of benznidazole, a drug currently used for the treatment of Chagas' disease. A panel of *in vitro* early ADME-Toxicity properties was assessed for this series of compounds and **19** yielded a satisfactory profile. The properties of compound **19** and miltefosine, a marketed drug, were compared. The specific assays included *h*ERG, cytochrome P450 (1A2, 2C9, 2C19, 2D6 and 3A4 isoforms), cell viability (A549 and WI38 cell-lines) and mitochondrial toxicity. The early ADME-Toxicity evaluation has a significant value in compound characterization since it points out *in vitro* liabilities before moving to *in vivo* studies. The different cut-off values were selected on the basis of accepted and recognized profiles for the approved anti-leishmanial compounds. According to the target product profile (TPP) description [40] (Fig. 6 and Table S8 of the Supporting Information), the profiles of the two compounds, **19** and miltefosine, are comparable. Compound **19** has a profile suitable for selection and prioritization, inhibiting only one cytochrome isoform (CYP1A2 EC_{50} = 0.4 μM) and being slightly toxic for A549. However, the A549 appear to be very sensitive to antioxidants such as **19** and this might be the reason of its higher toxicity with respect to miltefosine. The toxicity against THP1 mammalian cells is lower than that of miltefosine. The main advantages of compound **19** over miltefosine are the higher synthetic tractability and its inability to induce spontaneous resistance. The flavonoid scaffold allows a rapid optimization process and the synthesis of a wide range of derivatives at a lower cost with respect to miltefosine (drug cost is a pivotal parameter for NTDs that affect resource-poor settings). Moreover, **19** has a broad spectrum of activity on trypanosomatidic parasites, being more active than miltefosine on *T. brucei* (EC_{50} = 0.8 and 34 μM, respectively).

A Cos-Seq [28] functional cloning approach [41] yielded populations with a tolerance against the IC_{50} of **19**, but not against higher concentrations. The resistance against **19** is not as easily attained as against compounds such as miltefosine or antimony-based drugs [26,42].

Pharmacokinetic studies indicated that compound **19** has a long half-life (IV: 63.2 h; PO: 46.9 h) and allowed to proceed **19** to *in vivo* studies. The efficacy trial in a hamster chronic model of infection showed a reduction of PB in the spleen, the main target organ. This occurred in spite of a low concentration of compound **19** in plasma, likely related with low hydrosolubility. CDs formulation did not significantly improve this feature and, given the absence of toxicity of this compound, other formulations will have to be evaluated. Finally, the environmental sensitivity of the fluorescence of compound **19** results in large changes in both steady-state and time-dependent properties following **19** binding to five test proteins. This observation can be exploited in future investigations of **19** intracellular targets and off-targets, a strong asset in the rational design of optimized derivatives, and in the understanding of its mode of action in *Leishmania* parasites.

In conclusion, compound **19** offers the potential to tackle drug resistance in *Leishmania*, showing a broad activity spectrum against Trypanosomatidic infections *in vitro* and not leading to spontaneous resistance as observed for miltefosine and antimonials drugs.

5. Material and methods

5.1. General experimental procedures

All commercial chemicals and solvents were reagent grade and were used without further purification. TLC monitored reaction progress on pre-coated silica gel 60 F254 plates (Merck), and visualization was accomplished with UV light (254 nm). ^{1}H and ^{13}C NMR spectra were recorded on a Bruker FT-NMR AVANCE 400. Chemical shifts are reported as δ values (ppm) referenced to residual solvent ($CHCl_3$ at δ 7.26 ppm, DMSO at δ 2.50 ppm, MeOD at δ 3.31 ppm); *J* values are given in Hz. When peak multiplicities are given, the following abbreviations are used: s, singlet; d, doublet; t, triplet; q, quartet; m, multiplet; br, broadened signal. Silica gel Merck (60–230 mesh) was used for column chromatography. Mass spectra were obtained on a 6520 Accurate-Mass QTOF LC/MS and 6310A Ion Trap LC-MS(n).

5.2. General procedures for synthesis of compounds

5.2.1. General procedure for the synthesis of biaryl aldehydes (*59* and *60*)

To a solution of 5.49 mmol of the aryl halide in 20 mL of water/ethanol (1:1), 5.49 mmol of phenyl boronic acid, 13.73 mmol of K_2CO_3 and 293 mg of Palladium on carbon (5 mol%) were added. The mixture was stirred for 5 h at 60 °C. Then the reaction mixture was filtered through Celite and concentrated in vacuum. The

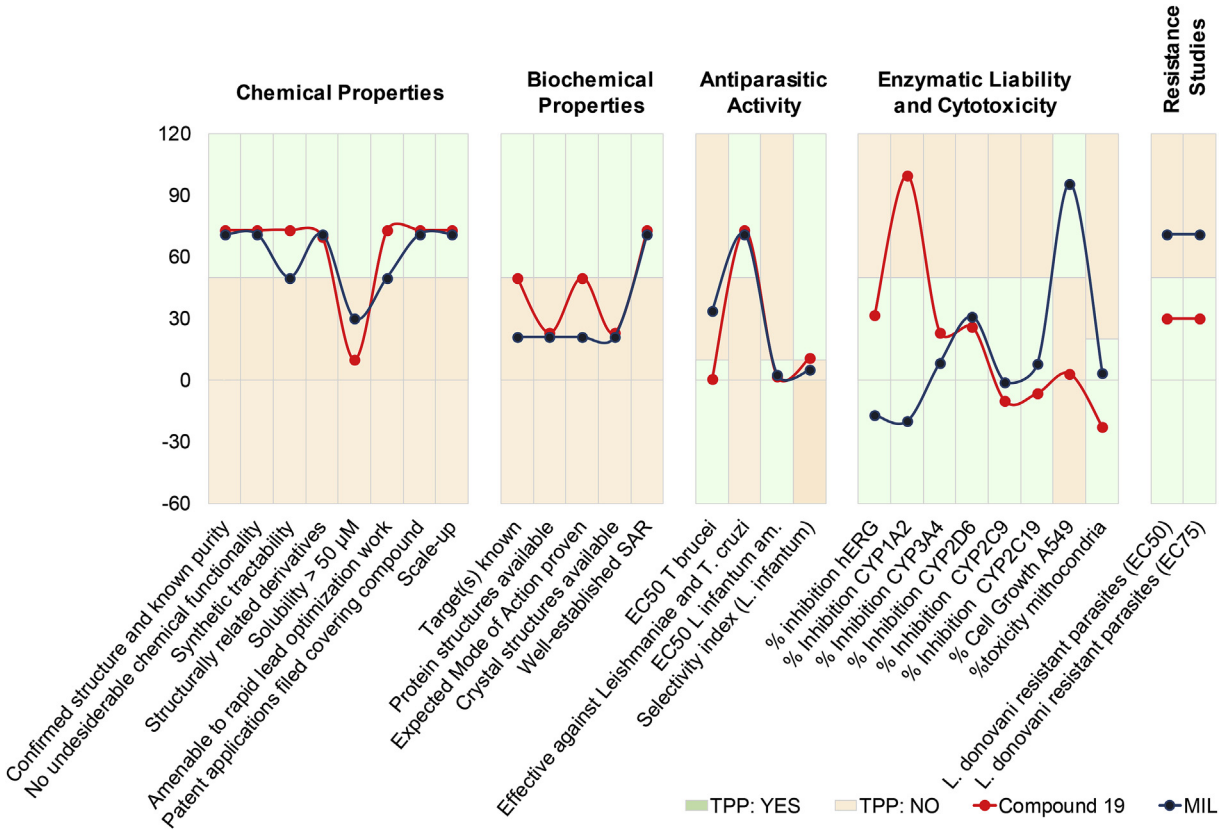

Fig. 6. Target product profile (TPP) of compound **19** (red line) and miltefosine (MIL) (blue line). For parameters requiring a yes/no answer, the cut-off was set at 50% of the y-axes. For parameters requiring a numeric value, the marker line between proper and improper behavior was set to the corresponding cut-off value described in the main text. Pale green color covers the area for which the compound parameters agree with the desired values, whereas pale red color covers the area with an improper profile. Red dots represent data relative to compound **19**, blue dots are related to MIL. Further details are reported in Table S8 of the Supporting Information. (For interpretation of the references to color in this figure legend, the reader is referred to the Web version of this article.)

mixture was extracted with ethyl acetate, the organic layer was dried over anhydrous sodium sulphate and evaporated under reduced pressure. The crude product was purified by column chromatography.

*5.2.2. General procedure for the synthesis of chalcones (**39**–**58**)*

An aqueous solution of NaOH (3 M, 1.6 mL) was added to a solution of aromatic ketone (1 mmol) and 3-methoxybenzaldehyde (1.2 eq), in EtOH (1–2 mL). The reaction was stirred at r.t for 18–24 h. The reaction mixture was cooled in an ice-water bath and acidified to pH 2 with concentrated HCl (37%). The solid formed was filtered, washed with ethanol and then further purified by recrystallization from ethanol. When no precipitate occurred, the reaction mixture was extracted with dichloromethane and washed with water and brine. The organic layer was dried over Na_2SO_4 and concentrated under reduced pressure. Column chromatography was then utilized to purify the desired product.

*5.2.3. General procedure for the synthesis of flavonol-like compounds (**1**, **2**, **5**, **6**, **8**, **9**, **11**, **13**, **14**, **16**–**20** and **22**–**32**)*

An aqueous solution of H_2O_2 (30%, 250 μL) was added to an ice-cold suspension of the chalcone (1 mmol) in ethanol (5 mL) and 1 M NaOH (2 mL). The mixture was allowed to warm at r.t. and was stirred overnight. Then the reaction mixture was cooled in an ice bath and distilled water (2–4 mL) was added. Concentrated HCl (37%) was added until pH 2. The solid formed was filtered, washed with ethanol and then further purified by recrystallization from ethanol. When no precipitate occurred, the reaction mixture was extracted with dichloromethane and washed with water and brine. The organic layer was dried over Na_2SO_4 and concentrated under reduced pressure. Column chromatography was then utilized to purify the desired product.

*5.2.4. General procedure for the synthesis of demethylated flavonol-like compounds (**3**, **4**, **7**, **10**, **12**, **15** and **21**)*

To a stirring solution of **14** (0.083 g, 0.205 mmol) in anhydrous dichloromethane (5 mL) under nitrogen at 0 °C, boron tribromide in dichloromethane (1.0 M, 1.85 mL, 1.847 mmol, 9 eq) was added. The mixture was allowed to warm at r.t. and was stirred for 2 days. The reaction mixture was then cooled to 0 °C and methanol (10 mL) was added. The reaction mixture was concentrated in vacuo. Water (10 mL) was added, the reaction sonicated and left to stand. The solid was filtered to give the pure product **15**.

(BBr_3 being widely used for the demethylation of methyl aryl ethers; 3 eq. of BBr_3 are used for each C–O bond cleavage).

*5.2.5. General procedure for the synthesis of esters and carbamates (**33**–**36**)*

To a suspension of **19** in dry DCM, triethylamine and an excess of acyl chloride was added. The mixture was stirred until the starting material was totally consumed (1–4 h). After basic workup, the crude was purified by column chromatography to obtain the desired product.

*5.2.6. General procedure for the synthesis of ethers (**37** and **38**)*

To a solution of **19** in dry DMF placed in a MW tube, K_2CO_3 (2.5

eq) and iodoethane/iodopropane (1.5 eq) was added. The mixture was irradiated with microwaves at 80 °C until the starting material was consumed. The mixture was subsequently filtered and concentrated and column chromatography was used to isolate the pure compound.

5.3. Synthesis of compounds

5.3.1. 2-(furan-2-yl)-3-hydroxy-6-methoxy-4H-chromen-4-one (**1**)

Compound **1** was prepared according to the general method for the synthesis of flavonol-like compounds reported above starting from compound **39**. Compound **1** was isolated as a yellow solid in 81% yield. mp: 197 °C. ^{1}H NMR ($CDCl_3$, 400 MHz) δ: 9.94 (br s, 1H), 8.03 (dd, J = 1.7, 0.7 Hz, 1H), 7.66 (d, J = 9.2, 1H), 7,45 (d, J = 3.1 Hz, 1H), 7.38 (dd, J = 9.1, 3.1 Hz, 1H), 7.28 (dd, J = 0.7, 3.5 Hz, 1H), 6.79 (dd, J = 3.5, 1.7 Hz, 1H), 3.88 (s, 3H). ^{13}C NMR ($CDCl_3$, 100 MHz) δ: 171.89, 156.49, 149.42, 145.62, 144.61, 139.66, 137.25, 123.71, 122.92, 120.28, 115.63, 113.26, 104.56, 56.19. ESI-HRMS calcd. for $C_{14}H_{11}O_5$ $[M+H]^+$ 258.0601, found 259.0611. Anal. calcd. for $C_{14}H_{10}O_5$: C, 65.12; H, 3.90; Found C, 65.34; H, 3.88.

5.3.2. 2-(furan-2-yl)-3-hydroxy-7-methoxy-4H-chromen-4-one (**2**)

Compound **2** was prepared according to the general method for the synthesis of flavonol-like compounds reported above starting from compound **40**. Compound **2** was isolated as a yellow solid in 23% yield. mp: 198 °C. ^{1}H NMR ($CDCl_3$, 400 MHz) δ: 9.87 (br s, 1H), 8.01 (dd, J = 1.8, 0.7 Hz, 1H), 8.00 (d, J = 8.9, 1H), 7,23 (dd, J = 0.7, 3.5 Hz, 1H), 7.19 (d, J = 2.3 Hz, 1H), 7.05 (dd, J = 8.9, 2.3 Hz, 1H), 6.79 (dd, J = 3.5, 1.8 Hz, 1H), 3.92 (s, 3H). ^{13}C NMR ($CDCl_3$, 100 MHz) δ: 171.78, 164.08, 156.46, 145.34, 144.62, 139.27, 137.35, 126.66, 116.13, 115.05 (2C), 113.22, 100.70, 56.58. ESI-HRMS calcd. for $C_{14}H_{11}O_5$ $[M+H]^+$ 258.0601, found 259.0606. Anal. calcd. for $C_{14}H_{10}O_5$: C, 65.12; H, 3.90; Found C, 65.17; H, 3.94.

5.3.3. 2-(furan-2-yl)-3,6-dihydroxy-4H-chromen-4-one (**3**)

Compound **3** was prepared according to the general method for the synthesis of demethylated flavonols reported above starting from compound **1**. Compound **3** was isolated as a yellow-brown solid in quantitative yield. mp 305 °C dec. ^{1}H NMR (DMSO, 400 MHz) δ: 9.89 (br s, 1H), 9.81 (br s, 1H), 8.02 (dd, J = 1.8, 0.8 Hz, 1H), 7.57 (d, J = 9.1, 0.3 Hz, 1H), 7.36 (dd, J = 3.0, 0.3 Hz, 1H), 7.26 (dd, J = 3.5, 0.8 Hz, 1H), 7.23 (dd, J = 9.1, 3.0 Hz, 1H), 6.78 (dd, J = 3.5, 1.8 Hz, 1H). ^{13}C NMR (DMSO, 100 MHz) δ: 171.97, 154.68, 148.46, 145.52, 144.71, 139.55, 137.01, 123.49, 123.13, 119.99, 115.48, 113.22, 107.45. ESI-HRMS calcd. for $C_{13}H_9O_5$ $[M+H]^+$ 245.0444, found 245.0446. Anal. calcd. for $C_{13}H_8O_5$: C, 63.94; H, 3.30; Found C, C, 63.69; H, 3.30.

5.3.4. 2-(furan-2-yl)-3,7-dihydroxy-4H-chromen-4-one (**4**)

Compound **4** was prepared according to the general method for the synthesis of demethylated flavonols reported above starting from compound **2**. Compound **4** was isolated as a gray solid in quantitative yield. mp: 285 °C. ^{1}H NMR (DMSO, 400 MHz) δ: 10.93 (br s, 1H), 9.74 (br s, 1H), 8.00 (dd, J = 1.8, 0.8 Hz, 1H), 7.95 (d, J = 8.7 Hz, 1H), 7.21 (dd, J = 3.5, 0.8 Hz, 1H), 6.92 (dd, J = 8.7, 2.2 Hz, 1H), 6.89 (d, J = 2.2 Hz, 1H), 6.77 (dd, J = 3.5, 1.8 Hz, 1H). ^{13}C NMR (DMSO, 100 MHz) δ: 171.79, 162.92, 156.47, 145.24, 144.70, 138.91, 137.09, 127.06, 115.28, 115.19, 114.85, 113.15, 102, 37. ESI-HRMS calcd. for $C_{13}H_9O_5$ $[M+H]^+$ 245.0444, found 245.0448. Anal. calcd. for $C_{13}H_8O_5$: C, 63.94; H, 3.30; Found C, C, 63.89; H, 3.33.

5.3.5. 3-hydroxy-6-methoxy-2-(4-methylthiophen-2-yl)-4H-chromen-4-one (**5**)

Compound **5** was prepared according to the general method for the synthesis of flavonol-like compounds reported above starting from compound **41**. Compound **5** was isolated as a yellow solid in 73% yield. mp: 200 °C. ^{1}H NMR ($CDCl_3$, 400 MHz) δ: 7.82 (d, J = 1.1 Hz, 1H), 7.55 (d, J = 3.1 Hz, 1H), 7.48 (d, J = 9.2, 1H), 7.28 (dd, J = 9.2, 3.1 Hz, 1H), 7.20 (m, 1H), 3.92 (s, 3H), 2.36 (d, J = 0.6 Hz, 3H). ^{13}C NMR ($CDCl_3$, 100 MHz) δ: 172.06, 156.48, 149.98, 142.76, 138.85, 136.00, 132.58, 131.52, 125.58, 124.00, 121.51, 119.50, 104.00, 55.93, 15.70. ESI-HRMS calcd. for $C_{15}H_{13}O_4S$ $[M+H]^+$ 289.0529, found 289.0529. Anal. calcd. for $C_{15}H_{12}O_4S$: C, 62.49; H, 4.20; S, 11.12; Found C, 62.43; H, 4.31; S, 11.09.

5.3.6. 3-hydroxy-7-methoxy-2-(4-methylthiophen-2-yl)-4H-chromen-4-one (**6**)

Compound **6** was prepared according to the general method for the synthesis of flavonol-like compounds reported above starting from compound **42**. Compound **6** was isolated as a brown solid in 29% yield. mp: 189 °C. ^{1}H NMR (DMSO, 400 MHz) δ: 10.02 (br s, 1H), 7.97 (d, J = 8.1 Hz, 1H), 7.75 (m, 1H), 7.46 (s, 1H), 7.19 (m, 1H), 7.02 (d, J = 8.1 Hz, 1H), 3.92 (s, 3H), 2.31 (s, 3H). ^{13}C NMR (DMSO, 100 MHz) δ: 171.89, 164.03, 156.47, 143.07, 138.15, 136.86, 132.62, 130.28, 126.59, 126.46, 116.05, 114.87, 100.59, 56.52. ESI-HRMS calcd. for $C_{15}H_{13}O_4S$ $[M+H]^+$ 289.0529, found 289.0529. Anal. calcd. for $C_{15}H_{12}O_4S$: C, 62.49; H, 4.20; S, 11.12; Found C, 62.79; H, 4.18; S, 10.92.

5.3.7. 3,6-dihydroxy-2-(4-methylthiophen-2-yl)-4H-chromen-4-one (**7**)

Compound **7** was prepared according to the general method for the synthesis of demethylated flavonols reported above starting from compound **5**. Compound **7** was isolated as a yellow solid in 91% yield. mp: 237 °C. ^{1}H NMR (DMSO, 400 MHz) δ: 9.97 (br s, 1H), 9.93 (br s, 1H), 7.76 (d, J = 1.2 Hz, 1H), 7.56 (d, J = 9.0 Hz, 1H), 7.47 (m, 1H), 7.35 (d, J = 3.0 Hz, 1H), 7.23 (dd, J = 9.0, 3.0 Hz, 1H), 2.30 (s, 3H). ^{13}C NMR (DMSO, 100 MHz) δ: 172.10, 154.58, 148.49, 143.37, 138.23, 136.59, 132.74, 130.61, 126.67, 123.41, 123.02, 119.84, 107.48, 15.75. ESI-HRMS calcd. for $C_{14}H_{11}O_4S$ $[M+H]^+$ 275.0373, found 275.0368. Anal. calcd. for $C_{14}H_{10}O_4S$: C, 61.31; H, 3.67; S, 11.69; Found C, 61.30; H, 3.67; S, 11.49.

5.3.8. 3-hydroxy-6-methyl-2-(4-methylthiophen-2-yl)-4H-chromen-4-one (**8**)

Compound **8** was prepared according to the general method for the synthesis of flavonol-like compounds reported above starting from compound **43**. Compound **8** was isolated as a yellow solid in 56% yield. mp: 222 °C. ^{1}H NMR (400 MHz, DMSO) δ: 10.10 (s, 1H), 7.88-7.86 (m, 1H), 7.76 (d, J = 1.3 Hz, 1H), 7.58 (d, J = 1.3 Hz, 2H), 7.48-7.46 (m, 1H), 2.43 (d, J = 0.5 Hz, 3H), 2.31 (s, 3H). ^{13}C NMR (100 MHz, DMSO) δ: 172.30, 152.89, 143.45, 138.24, 137.12, 135.23, 134.46, 132.58, 130.69, 126.83, 124.37, 121.92, 118.31, 20.86, 15.74. ESI-HRMS calcd. for $C_{15}H_{13}O_3S$ $[M+H]^+$ 273.0580, found 273.0583. Anal. calcd. for $C_{15}H_{12}O_3S$: C, 66.16; H, 4.44; S, 11.77; Found C, 65.98; H, 4.42; S, 11.70.

5.3.9. 3-hydroxy-5-methoxy-2-(4-methylthiophen-2-yl)-4H-chromen-4-one (**9**)

Compound **9** was prepared according to the general method for the synthesis of flavonol-like compounds reported above starting from compound **44**. Compound **9** was isolated as a yellow solid in 25% yield. mp: 170−171 °C. ^{1}H NMR (DMSO, 400 MHz) δ: 9.71 (br s, 1H), 7.71 (d, J = 1.4 Hz, 1H), 7.66 (t, J = 8.4 Hz, 1H), 7.45 (m, 1H), 7.19 (dd, J = 8.4, 0.7 Hz, 1H), 7.95 (d, J = 8.4 Hz, 1H), 3.94 (s, 3H), 2.30 (s, 3H). ^{13}C NMR (DMSO, 100 MHz) δ: 171.74, 159.67, 156.59, 140.71, 138.23, 137.36, 134.37, 132.40, 130.16, 126.25, 112.59, 110.20, 106.44, 56.69, 15.76. ESI-HRMS calcd. for $C_{15}H_{13}O_4S$ $[M+H]^+$ 289.0529, found 289.0532. Anal. calcd. for $C_{15}H_{12}O_4S$: C, 62.49; H, 4.20; S, 11.12; Found C, 62.71; H, 4.24; S, 11.17.

*5.3.10. 3,5-dihydroxy-2-(4-methylthiophen-2-yl)-4H-chromen-4-one (**10**)*

Compound **10** was prepared according to the general method for the synthesis of demethylated flavonols reported above starting from compound **9**. Compound **10** was isolated as a green solid in 79% yield. mp: 180–181 °C. ^{1}H NMR (DMSO, 400 MHz) δ: 12.36 (br s, 1H), 10.44 (br s, 1H), 7.81 (d, J = 1.3 Hz, 1H), 7.62 (t, J = 8.3 Hz, 1H), 7.54 (m, 1H), 7.11 (dd, J = 8.3, 0.6 Hz, 1H), 6.77 (dd, J = 8.3, 0.6 Hz, 1H), 2.31 (s, 3H). ^{13}C NMR (DMSO, 100 MHz) δ: 176.38, 159.40, 154.28, 144.85, 137.93, 135.24, 135.22, 131.40, 130.99, 127.47, 109.53, 109.43, 107.25, 15.20. ESI-HRMS calcd. for $C_{14}H_{11}O_4S$ $[M+H]^+$ 275.0373, found 289.0375. Anal. calcd. for $C_{14}H_{10}O_4S$: C, 61.31; H, 3.67; S, 11.69; Found C, 61.01; H, 3.56; S, 11.41.

*5.3.11. 3-hydroxy-7-methoxy-2-(3-methylthiophen-2-yl)-4H-chromen-4-one (**11**)*

Compound **11** was prepared according to the general method for the synthesis of flavonol-like compounds reported above starting from compound **45**. Compound **11** was isolated as a brown solid in 25% yield. mp: 177–178 °C. ^{1}H NMR (DMSO, 400 MHz) δ: 9.69 (br s, 1H), 7.99 (d, J = 8.8 Hz, 1H), 7.75 (d, J = 4.9 Hz, 1H), 7.11 (m, 1H), 7.06-7.03 (m, 2H), 3.91 (s, 3H), 2.54 (s, 3H). ^{13}C NMR (DMSO, 100 MHz) δ: 171.99, 164.01, 156.66, 144.10, 139.70, 137.67, 131.66, 129.43, 126.62, 125.98, 116.05, 114.98, 100.49, 56.55, 17.03. ESI-HRMS calcd. for $C_{15}H_{13}O_4S$ $[M+H]^+$ 289.0529, found 289.0525. Anal. calcd. for $C_{15}H_{12}O_4S$: C, 62.49; H, 4.20; S, 11.12; Found C, 62.53; H, 4.11; S, 11.05.

*5.3.12. 3,7-dihydroxy-2-(3-methylthiophen-2-yl)-4H-chromen-4-one (**12**)*

Compound **12** was prepared according to the general method for the synthesis of demethylated flavonols reported above starting from compound **11**. Compound **12** was isolated as a yellow solid in 92% yield. mp: 278 °C dec. ^{1}H NMR (DMSO, 400 MHz) δ: 10.74 (br s, 1H), 9.58 (br s, 1H), 7.94 (d, J = 8.8 Hz, 1H), 7.74 (d, J = 5.0 Hz, 1H), 7.05 (d, J = 5.0 Hz, 1H), 6.92 (dd, J = 8.8, 2.2 Hz, 1H), 6.86 (d, J = 2.2 Hz, 1H), 2.51 (s, 1H). ^{13}C NMR (DMSO, 100 MHz) δ: 172.00, 162.83, 156.66, 143.69, 139.45, 137.39, 131.65, 129.30, 127.01, 126.12, 115.27, 115.10, 102.21, 16.91. ESI-HRMS calcd. for $C_{14}H_{11}O_4S$ $[M+H]^+$ 275.0373, found 289.0375. Anal. calcd. for $C_{14}H_{10}O_4S$: C, 61.31; H, 3.67; S, 11.69; Found C, 60.99; H, 4.00; S, 11.23.

*5.3.13. 3-hydroxy-6-methyl-2-(5-methylthiophen-2-yl)-4H-chromen-4-one (**13**)*

Compound **13** was prepared according to the general method for the synthesis of flavonol-like compounds reported above starting from compound **46**. Compound **13** was isolated as a yellow solid in 60% yield. mp: 185–186 °C.^{1}H NMR (400 MHz, DMSO) δ: 9.79 (s, 1H), 7.91-7.87 (m, 1H), 7.77 (d, J = 5.0 Hz, 1H), 7.62-7.56 (m, 2H), 7.07 (d, J = 5.0 Hz, 1H), 2.55 (s, 3H), 2.44 (s, 3H). ^{13}C NMR (100 MHz, DMSO) δ: 172.40, 153.06, 144.73, 139.98, 137.82, 135.20, 134.54, 131.75, 129.80, 125.92, 124.32, 121.89, 118.35, 20.89, 17.08. ESI-HRMS calcd. for $C_{15}H_{13}O_3S$ $[M+H]^+$ 273.0580, found 273.0585. Anal. calcd. for $C_{15}H_{12}O_3S$: C, 66.16; H, 4.44; S, 11.77; Found C, 66.08; H, 4.31; S, 11.80.

*5.3.14. 2-(3′,4′-dimethoxy-[1,1′-biphenyl]-3-yl)-3-hydroxy-6-methoxy-4H-chromen-4-one (**14**)*

The intermediate chalcone was synthesized following the general method for the synthesis of (2E)-1-(2-hydroxyphenyl)-3-phenylprop-2-en-1-ones and was used, without further purification, for the synthesis of compound **14** according to the general method for the synthesis of flavonol-like compounds reported above. Compound **14** was isolated as a yellow solid in quantitative yield. mp: 182–183 °C. ^{1}H NMR (DMSO, 400 MHz) δ: 9.63 (br s, 1H), 8.42 (s, 1H), 8.14 (d, J = 8.0 Hz, 1H), 7.79 (d, J = 9.1 Hz, 1H), 7.79 (m, 1H), 7.63 (t, J = 8.0 Hz, 1H), 7.47 (d, J = 3.0 Hz, 1H), 7.43 (dd, J = 9.1, 3.0 Hz, 1H), 7.28 (s, 1H), 7.25 (dd, J = 8.3, 1.9 Hz, 1H), 7.09 (d, J = 8.3 Hz, 1H), 3.90 (s, 3H), 3.87 (s, 3H), 3.82 (s, 3H). ^{13}C NMR (DMSO, 100 MHz) δ: 173.00, 156.47, 150.12, 149.63, 149.28, 145.69, 140.98, 139.23, 133.07, 132.40, 129.47, 128.45, 126. 60, 126.12, 124.06, 122.39, 120.74, 119.57, 112.78, 111.17, 104.30, 56.21, 56.11, 56.12. ESI-HRMS calcd. for $C_{24}H_{21}O_6$ $[M+H]^+$ 405.1333, found 405.1339. Anal. calcd. for $C_{24}H_{20}O_6$: C, 71.28; H, 4.98; Found C, 71.35; H, 4.86.

*5.3.15. 2-(3′,4′-dihydroxy-[1,1′-biphenyl]-3-yl)-3,6-dihydroxy-4H-chromen-4-one (**15**)*

Compound **15** was prepared according to the general method for the synthesis of demethylated flavonols reported above starting from compound **14**. Compound **15** was isolated as a brown solid in 84% yield. mp: 302–303 °C dec. ^{1}H NMR (DMSO, 400 MHz) δ: 9.97 (br s, 1H), 9.43 (br s, 1H), 9.11 (br s, 2H), 8.33 (s, 1H), 8.07 (d, J = 7.9 Hz, 1H), 7.67 (d, J = 9.1 Hz, 1H), 7.64 (d, J = 7.9 Hz, 1H), 7.58 (t, J = 7.7 Hz, 1H), 7.38 (d, J = 3.0 Hz, 1H), 7.27 (dd, J = 3.0, 9.1 Hz, 1H), 7.09 (d, J = 2.2 Hz, 1H), 7.00 (dd, J = 8.2, 2.2 Hz, 1H), 7.86 (d, J = 8.2 Hz, 1H). ^{13}C NMR (DMSO, 100 MHz) δ: 173.00, 154.61, 149.52, 149.12, 146.16, 145.96, 145.55, 145.39, 144.35, 141.18, 138.92, 132.43, 131.60, 129.44, 127.89, 125.99, 125.69, 123.77, 122.58, 120.41, 118.31, 116.57, 114.54, 107.43. ESI-HRMS calcd. for $C_{21}H_{15}O_6$ $[M+H]^+$ 363.0863, found 363.0865. Anal. calcd. for $C_{21}H_{14}O_6$: C, 69.61; H, 3.89; Found C, 69.35; H, 4.01.

*5.3.16. 2-(3-(benzo[d] [1,3]dioxol-5-yl)phenyl)-3-hydroxy-6-methoxy-4H-chromen-4-one (**16**)*

The intermediate chalcone was synthesized following the general method for the synthesis of (2E)-1-(2-hydroxyphenyl)-3-phenylprop-2-en-1-ones and was used, without further purification, for the synthesis of compound **16** according to the general method for the synthesis of flavonol-like compounds reported above. Compound **16** was isolated as a brown solid in 38% yield. mp: 226 °C. ^{1}H NMR (400 MHz, DMSO) δ: 9.60 (s, 1H), 8.39 (s, 1H), 8.16 (d, J = 7.9 Hz, 1H), 7.81 (d, J = 9.1 Hz, 1H), 7.73 (d, J = 7.8 Hz, 1H), 7.62 (t, J = 7.8 Hz, 1H), 7.47 (d, J = 3.0 Hz, 1H), 7.43 (dd, J = 9.1, 3.0 Hz, 1H), 7.31 (d, J = 1.3 Hz, 1H), 7.22 (d, J = 8.0 Hz, 1H), 7.06 (d, J = 8.0 Hz, 1H), 6.10 (s, 2H), 3.90 (s, 3H). ^{13}C NMR (100 MHz, DMSO) δ: 173.05, 156.45, 150.10, 148.53, 147.60, 145.50, 140.70, 139.25, 134.54, 132.42, 129.53, 128.44, 126.74, 126.11, 124.04, 122.35, 120.98, 120.75, 109.23, 107.75, 104.27, 101.71, 56.21. ESI-HRMS calcd. for $C_{23}H_{17}O_6$ $[M+H]^+$ 389.1020, found 389.1026. Anal. calcd. for $C_{23}H_{16}O_6$: C, C, 71.13; H, 4.15; Found C, 71.06; H, 4.17.

*5.3.17. 2-(benzo[d] [1,3]dioxol-5-yl)-3-hydroxy-7-methoxy-4H-chromen-4-one (**17**)*

Compound **17** was prepared according to the general method for the synthesis of flavonol-like compounds reported above starting from compound **47**. Compound **17** was isolated as a yellow solid in 52% yield. mp: 211 °C. ^{1}H NMR (400 MHz, DMSO) δ: 9.39 (br s, 1H), 7.98 (d, J = 8.9 Hz, 1H), 7.84 (dd, J = 8.4, 1.7 Hz, 1H), 7.77 (d, J = 1.7 Hz, 1H), 7.32 (d, J = 2.4 Hz, 1H), 7.12 (d, J = 8.4 Hz, 1H), 7.04 (dd, J = 8.9, 2.4 Hz, 1H), 6.14 (s, 2H), 3.92 (s, 3H). ^{13}C NMR (100 MHz, DMSO) δ: 172.58, 164.04, 156.79, 148.80, 148.00, 144.87, 138.44, 126.51, 125.65, 122.90, 115.56, 115.03, 108.89, 107.75, 102.10, 100.82, 56.54. ESI-HRMS calcd. for $C_{17}H_{13}O_6$ $[M+H]^+$ 313.0707, found 313.0704. Anal. calcd. for $C_{17}H_{12}O_6$: C, 65.39; H, 3.87; Found C, 65.51; H, 3.75.

*5.3.18. 3-hydroxy-6-methoxy-2-(quinolin-6-yl)-4H-chromen-4-one (**18**)*

The intermediate chalcone was synthesized following the general method for the synthesis of (2E)-1-(2-hydroxyphenyl)-3-

phenylprop-2-en-1-ones and was used, without further purification, for the synthesis of compound **18** according to the general method for the synthesis of flavonol-like compounds reported above. Compound **18** was isolated as a yellow solid in 64% yield. mp 280–281 °C. ^{1}H NMR (400 MHz, DMSO) δ: 10.03 (s, 1H), 9.16 (dd, J = 4.7, 1.5 Hz, 1H), 9.00 (d, J = 1.8 Hz, 1H), 8.91 (d, J = 8.3 Hz, 1H), 8.73 (dd, J = 9.1, 1.9 Hz, 1H), 8.38 (d, J = 9.1 Hz, 1H), 7.87 (dd, J = 8.3, 4.7 Hz, 1H), 7.82-7.77 (m, 1H), 7.49-7.44 (m, 2H), 3.90 (s, 3H). ^{13}C NMR (100 MHz, DMSO) δ: 173.17, 156.52, 150.14, 148.75, 143.76, 143.22, 142.32, 140.20, 131.57, 131.09, 128.61, 128.47, 124.95, 124.45, 123.07, 122.36, 120.63, 104.29, 56.24. ESI-HRMS calcd. for $C_{19}H_{14}NO_4$ $[M+H]^+$ 320.0917, found 320.0910. Anal. calcd. for $C_{19}H_{13}NO_4$: C, 71.47; H, 4.10; N, 4.39; Found C, 71.30; H, 4.16; N, 4.37.

5.3.19. 2-(benzo[b]thiophen-3-yl)-3-hydroxy-6-methoxy-4H-chromen-4-one (**19**)

The intermediate chalcone was synthesized following the general method for the synthesis of (2E)-1-(2-hydroxyphenyl)-3-phenylprop-2-en-1-ones and was used, without further purification, for the synthesis of compound **19** according to the general method for the synthesis of flavonol-like compounds reported above. Compound **19** was isolated as a yellow solid in 40% yield. mp: 216–217 °C. ^{1}H NMR (400 MHz, DMSO) δ: 9.63 (s, 1H), 8.62 (s, 1H), 8.39 (d, J = 7.8 Hz, 1H), 8.12 (d, J = 7.8 Hz, 1H), 7.78 (d, J = 9.0 Hz, 1H), 7.55 - 7.43 (m, 4H), 3.90 (s, 3H). ^{13}C NMR (100 MHz, DMSO) δ: 172.48, 156.55, 149.70, 144.68, 139.58, 139.01, 136.90, 132.60, 126.33, 125.61, 125.37, 124.85, 123.83, 123.51, 122.76, 120.44, 104.43, 56.22. ESI-HRMS calcd. for $C_{18}H_{13}O_4S$ $[M+H]^+$ 325.0529, found 325.0531. Anal. calcd. for $C_{18}H_{12}O_4S$: C, 66.66; H, 3.73; S, 9.88; Found C, 66.45; H, 3.75; S, 9.75.

5.3.20. 3-hydroxy-2-(1H-indol-3-yl)-6-methoxy-4H-chromen-4-one (**20**)

Compound **20** was prepared according to the general method for the synthesis of flavonol-like compounds reported above starting from compound **48**. Compound **20** was isolated as a yellow solid in 54% yield. mp: 273 °C dec. ^{1}H NMR (400 MHz, DMSO) δ: 11.96 (br s, 1H), 9.36 (br s, 1H), 8.44-8.40 (m, 1H), 8.36 (d, J = 2.8 Hz, 1H), 7.87 (d, J = 9.1 Hz, 1H), 7.57-7.53 (m, 1H), 7.49 (d, J = 3.0 Hz, 1H), 7.37 (dd, J = 9.1, 3.0 Hz, 1H), 7.29-7.23 (m, 2H), 3.90 (s, 3H). ^{13}C NMR (100 MHz, DMSO) δ: 170.55, 156.35, 149.30, 148.48, 136.57, 136.18, 130.79, 125.03, 123.00, 122.98, 122.54, 122.14, 121.43, 120.08, 112.72, 106.82, 104.61, 56.15. ESI-HRMS calcd. for $C_{18}H_{14}NO_4$ $[M+H]^+$ 308.0917, found 308.0915. Anal. calcd. for $C_{18}H_{13}NO_4$: C, 70.35; H, 4.26; N, 4.56; Found C, 70.45; H, 4.18; N, 4.51.

5.3.21. 3,6-dihydroxy-2-(1H-indol-3-yl)-4H-chromen-4-one (**21**)

Compound **21** was prepared according to the general method for the synthesis of demethylated flavonols reported above starting from compound **20**. Compound **21** was isolated as a yellow solid in 92% yield. Mp: 305 °C. ^{1}H NMR (400 MHz, DMSO) δ 11.94 (s, 1H), 9.87 (s, 1H), 9.22 (s, 1H), 8.40 (dd, J = 6.6, 2.2 Hz, 1H), 8.34 (d, J = 2.9 Hz, 1H), 7.76 (d, J = 9.0 Hz, 1H), 7.55 (dd, J = 6.6, 2.2 Hz, 1H), 7.40 (d, J = 3.0 Hz, 1H), 7.27-7.23 (m, 1H), 7.24 (d, J = 7.4 Hz, 1H), 7.22 (d, J = 9.0, 3.0 Hz, 1H). ^{13}C NMR (100 MHz, DMSO) δ: 170.18, 153.98, 147.89, 147.83, 136.08, 135.48, 130.17, 124.57, 122.71, 122.45, 121.88, 121.61, 120.89, 119.24, 112.21, 107.00, 106.42. ESI-HRMS calcd. for $C_{17}H_{12}NO_4$ $[M+H]^+$ 294.0761, found 294.0763. Anal. calcd. for $C_{17}H_{11}NO_4$: C, 69.62; H, 3.78; N, 4.78; Found C, 69.49; H, 3.96; N, 4.68.

5.3.22. 3-hydroxy-6-methoxy-2-(1-methyl-1H-indol-3-yl)-4H-chromen-4-one (**22**)

The intermediate chalcone was synthesized following the general method for the synthesis of (2E)-1-(2-hydroxyphenyl)-3-phenylprop-2-en-1-ones and was used, without further purification, for the synthesis of compound **22** according to the general method for the synthesis of flavonol-like compounds reported above. Compound **22** was isolated as a yellow solid in 60% yield. mp: 290–293 °C. ^{1}H NMR (400 MHz, DMSO) δ: 9.41 (br s, 1H), 8.43 (dd, J = 7.2, 0.9 Hz, 1H), 8.35 (s, 1H), 7.87 (d, J = 9.1 Hz, 1H), 7.59 (d, J = 7.7 Hz, 1H), 7.48 (d, J = 3.1 Hz, 1H), 7.37 (dd, J = 9.1, 3.1 Hz, 1H), 7.35 (m, 1H), 7.31 (m, 1H), 7.28 (dd, J = 7.2, 1.1 Hz, 1H), 3.94 (s, 3H), 3.89 (s, 3H). ^{13}C NMR (100 MHz, DMSO) δ: 170.54, 156.36, 149.28, 148.13, 137.13, 136.15, 134.40, 125.44, 123.07, 123.01, 122.53, 122.35, 121.70, 120.08, 111.06, 105.87, 104.64, 56.17, 33.61. ESI-HRMS calcd. for $C_{19}H_{16}NO_4$ $[M+H]^+$ 322.1074, found 322.1072. Anal. calcd. for $C_{19}H_{15}NO_4$: C, 71.02; H, 4.71; N, 4.36; Found C, 71.13; H, 4.70; N, 4.19.

5.3.23. 2-(benzo[b]thiophen-3-yl)-3-hydroxy-6-methyl-4H-chromen-4-one (**23**)

Compound **23** was prepared according to the general method for the synthesis of flavonol-like compounds reported above starting from compound **49**. Compound **23** was isolated as a pale yellow solid in 41% yield. mp: 236–237 °C. ^{1}H NMR (400 MHz, DMSO) δ: 9.64 (s, 1H), 8.62 (s, 1H), 8.39 (dd, J = 7.4, 0.9 Hz, 1H), 8.12 (dd, J = 7.2, 0.9 Hz, 1H), 7.95 (d, J = 0.9 Hz, 1H), 7.71 (d, J = 8.7 Hz, 1H), 7.64 (dd, J = 8.7, 2.1 Hz, 1H), 7.57 - 7.51 (m, 1H), 7.51-7.45 (m, 1H), 2.46 (s, 3H). ^{13}C NMR (100 MHz, DMSO) δ: 172.28, 152.62, 144.17, 139.10, 138.84, 136.41, 134.83, 134.18, 132.14, 125.84, 125.11, 124.88, 124.36, 123.88, 123.02, 121.39, 118.08, 20.41. ESI-HRMS calcd. for $C_{18}H_{13}O_3S$ $[M+H]^+$ 309.0580, found 309.0582. Anal. calcd. for $C_{18}H_{12}O_3S$: C, 70.11; H, 3.92; S, 10.40; Found C, 70.28; H, 3.91; S, 10.31.

5.3.24. 2-(benzo[b]thiophen-3-yl)-6-bromo-3-hydroxy-4H-chromen-4-one (**24**)

Compound **24** was prepared according to the general method for the synthesis of flavonol-like compounds reported above starting from compound **50**. Compound **24** was isolated as a yellow solid in 66% yield. mp: 251 °C. ^{1}H NMR (400 MHz, DMSO) δ: 9.90 (s, 1H), 8.65 (s, 1H), 8.39 (dd, J = 7.3, 1.2 Hz, 1H), 8.23 (d, J = 2.5 Hz, 1H), 8.12 (dd, J = 7.3, 1.2 Hz, 1H), 7.96 (dd, J = 9.0, 2.5 Hz, 1H), 7.83 (d, J = 9.0 Hz, 1H), 7.56-7.46 (m, 2H). ^{13}C NMR (100 MHz, DMSO) δ: 171.69, 153.63, 145.36, 139.60, 139.57, 136.78, 136.53, 133.17, 127.23, 126.01, 125.62, 125.40, 124.89, 123.79, 123.49, 121.51, 117.46. ESI-HRMS calcd. for $C_{17}H_{11}O_3SBr^{79}$ $[M+H]^+$ 372.9529, found 372.9525. Calcd for $C_{17}H_{11}O_3SBr^{81}$ $[M+H]^+$ 374.9509, found 374.9498. Anal. calcd. for $C_{17}H_9BrO_3S$: C, 54.71; H, 2.43; S, 8.59; Found C, 54.85; H, 2.41; S, 8.57.

5.3.25. 2-(benzo[b]thiophen-3-yl)-6-fluoro-3-hydroxy-4H-chromen-4-one (**25**)

Compound **25** was prepared according to the general method for the synthesis of flavonol-like compounds reported above starting from compound **51**. Compound **25** was isolated as a pale yellow solid in 70% yield. mp: 236 °C. ^{1}H NMR (400 MHz, DMSO) δ: 9.81 (br s, 1H), 8.64 (s, 1H), 8.38 (d, J = 7.5 Hz, 1H), 8.12 (d, J = 7.5 Hz, 1H), 7.91 (dd, J = 9.2, 4.2 Hz, 1H), 7.81 (dd, J = 8.5, 3.1 Hz, 1H), 7.74-7.69 (m, 1H), 7.55 - 7.46 (m, 2H). ^{13}C NMR (100 MHz, DMSO) δ: 171.74 (d, J = 2.4 Hz), 158.52 (d, J = 243.5 Hz), 150.75, 144.80, 139.08, 138.62, 136.33, 132.59, 125.59, 125.14, 124.91, 124.39, 123.01, 122.72 (d, J = 7.6 Hz), 121.86 (d, J = 25.8 Hz), 121.12 (d, J = 8.5 Hz), 109.01 (d, J = 23.7 Hz). ESI-HRMS calcd. for $C_{17}H_{10}FO_3S$ $[M+H]^+$ 313.0329, found 313.0329. Anal. calcd. for $C_{17}H_9FO_3S$: C, 65.38; H, 2.90; S, 10.27; Found C, 65.19; H, 2.86; S, 10.17.

*5.3.26. 2-(benzo[b]thiophen-3-yl)-6-chloro-3-hydroxy-4H-chromen-4-one (**26**)*

Compound **26** was prepared according to the general method for the synthesis of flavonol-like compounds reported above starting from compound **52**. Compound **26** was isolated as a yellow solid in 63% yield. mp: 253–254 °C. ^{1}H NMR (400 MHz, DMSO) δ: 9.89 (br s, 1H), 8.65 (s, 1H), 8.38 (d, J = 7.5 Hz, 1H), 8.12 (d, J = 7.5 Hz, 1H), 8.08 (d, J = 2.5 Hz, 1H), 7.89 (d, J = 9.0 Hz, 1H), 7.84 (dd, J = 9.0, 2.5 Hz, 1H), 7.56-7.46 (m, 2H). ^{13}C NMR (100 MHz, DMSO) δ: 171.34, 152.78, 144.87, 139.08, 139.06, 136.30, 133.39, 132.71, 129.12, 125.51, 125.15, 124.93, 124.41, 123.60, 123.02, 122.85, 120.85. ESI-HRMS calcd. For $C_{17}H_{10}O_3SCl^{35}$ $[M+H]^+$ 329.0034, found 329.0036. calcd. for $C_{17}H_{10}O_3SCl^{37}$ $[M+H]^+$ 331.0005, found 331.0007. Anal. calcd. for $C_{17}H_9ClO_3S$: C, 62.11; H, 2.76; S, 9.75; Found C, 62.33; H, 2.73; S, 9.63.

*5.3.27. 2-(benzo[b]thiophen-3-yl)-3-hydroxy-4H-chromen-4-one (**27**)*

Compound **27** was prepared according to the general method for the synthesis of flavonol-like compounds reported above starting from compound **53**. Compound **27** was isolated as a pale brown solid in 37% yield. mp: 225 °C. ^{1}H NMR (400 MHz, DMSO) δ: 9.70 (s, 1H), 8.63 (s, 1H), 8.40 (m, 1H), 8.19-8.11 (m, 2H), 7.85-7.80 (m, 2H), 7.57-7.47 (m, 3H). ^{13}C NMR (100 MHz, DMSO) δ: 172.41, 154.30, 144.33, 139.11, 138.92, 136.41, 133.61, 132.27, 125.79, 125.13, 124.90, 124.83, 124.69, 124.36, 123.04, 121.71, 118.31. ESI-HRMS calcd. for $C_{17}H_{11}O_3S$ $[M+H]^+$ 295.0423, found 295.0426. Anal. calcd. for $C_{17}H_{10}O_3S$: C, 69.37; H, 3.42; S, 10.89; Found C, 69.18; H, 3.43; S, 10.87.

*5.3.28. 2-(benzo[b]thiophen-3-yl)-3-hydroxy-7-methoxy-4H-chromen-4-one (**28**)*

Compound **28** was prepared according to the general method for the synthesis of flavonol-like compounds reported above starting from compound **54**. Compound **28** was isolated as a yellow solid in 12% yield. mp: 236 °C. ^{1}H NMR (400 MHz, DMSO) δ: 9.54 (s, 1H), 8.57 (s, 1H), 8.39 (d, J = 7.8 Hz, 1H), 8.12 (d, J = 7.8 Hz, 1H), 8.06 (d, J = 8.9 Hz, 1H), 7.61-7.44 (m, 2H), 7.28 (d, J = 2.2 Hz, 1H), 7.09 (dd, J = 8.9, 2.2 Hz, 1H), 3.95 (s, 3H). ^{13}C NMR (100 MHz, DMSO) δ: 171.84, 163.62, 156.24, 143.70, 139.09, 138.62, 136.40, 131.66, 126.19, 125.87, 125.10, 124.85, 124.44, 122.99, 115.56, 114.69, 100.22, 56.15. ESI-HRMS calcd. for $C_{18}H_{13}O_4S$ $[M+H]^+$ 325.0529, found 325.0526. Anal. calcd. for $C_{18}H_{12}O_4S$: C, 66.66; H, 3.73; S, 9.88; Found C, 66.90; H, 3.64; S, 9.72.

*5.3.29. 2-(benzo[b]thiophen-3-yl)-3-hydroxy-7-methyl-4H-chromen-4-one (**29**)*

Compound **29** was prepared according to the general method for the synthesis of flavonol-like compounds reported above starting from compound **55**. Compound **29** was isolated as a brown solid in 21% yield. mp: 237 °C. ^{1}H NMR (400 MHz, DMSO) δ: 9.62 (s, 1H), 8.62 (s, 1H), 8.42-8.40 (m, 1H), 8.13 (d, J = 7.7 Hz, 1H), 8.05 (d, J = 7.8 Hz, 1H), 7.67-7.47 (m, 1H, 3H), 7.33 (d, J = 7.8 Hz, 1H), 2.51 (s, 1H). ^{13}C NMR (100 MHz, DMSO) δ: 172.23, 154.41, 144.60, 143.94, 139.12, 138.77, 136.43, 132.06, 126.22, 125.81, 125.11, 124.89, 124.60, 124.38, 123.03, 119.48, 117.73, 21.21. ESI-HRMS calcd. for $C_{18}H_{13}O_3S$ $[M+H]^+$ 309.0580, found 309.0586. Anal. calcd. for $C_{18}H_{12}O_3S$: C, 70.11; H, 3.92; S, 10.40; Found C, 69.95; H, 4.11; S, 9.21.

*5.3.30. 2-(benzo[b]thiophen-3-yl)-7-fluoro-3-hydroxy-4H-chromen-4-one (**30**)*

Compound **30** was prepared according to the general method for the synthesis of flavonol-like compounds reported above starting from compound **56**. Compound **30** was isolated as a yellow solid in 70% yield. mp: 258 °C. ^{1}H NMR (400 MHz, DMSO) δ: 9.78 (br s, 1H), 8.62 (s, 1H), 8.39 (d, J = 7.5 Hz, 1H), 8.22 (dd, J = 8.9, 6.4 Hz, 1H), 8.12 (d, J = 7.5 Hz, 1H), 7.81 (dd, J = 9.8, 2.3 Hz, 1H), 7.55-7.47 (m, 2H), 7.40 (td, J = 8.9, 2.3 Hz, 1H). ^{13}C NMR (100 MHz, DMSO) δ: 171.83, 164.80 (d, J = 251.3 Hz), 155.25 (d, J = 14.2 Hz), 144.76, 139.07, 138.92, 136.32, 132.27, 127.63 (d, J = 11.0 Hz), 125.56, 125.16, 124.91, 124.53, 122.98, 118.95, 113.62 (d, J = 23.3 Hz), 104.95 (d, J = 25.6 Hz). ESI-HRMS calcd. for $C_{17}H_{10}FO_3S$ $[M+H]^+$ 313.0329, found 313.0323. Anal. calcd. for $C_{17}H_9FO_3S$: C, 65.38; H, 2.90; S, 10.27; Found C, 65.35; H, 2.88; S, 10.04.

*5.3.31. 2-(benzo[b]thiophen-3-yl)-7-chloro-3-hydroxy-4H-chromen-4-one (**31**)*

Compound **31** was prepared according to the general method for the synthesis of flavonol-like compounds reported above starting from compound **57**. Compound **31** was isolated as a yellow solid in 69% yield. mp: 267–268 °C. ^{1}H NMR (400 MHz, DMSO) δ: 9.85 (s, 1H), 8.64 (s, 1H), 8.43 (d, J = 7.8 Hz, 1H), 8.18-8.10 (m, 2H), 8.05 (s, 1H), 7.58-7.46 (m, 3H). ^{13}C NMR (100 MHz, DMSO) δ: 171.82, 154.41, 144.66, 139.13, 139.05, 137.99, 136.31, 132.58, 126.67, 125.49, 125.28, 125.23, 124.94, 124.66, 122.97, 120.63, 118.26. ESI-HRMS calcd. for $C_{17}H_{10}O_3SCl^{35}$ $[M+H]^+$ 329.0034, found 329.0036. Calcd for $C_{17}H_{10}O_3SCl^{37}$ $[M+H]^+$331.0005, found 331.0007. Anal. calcd. for $C_{17}H_9ClO_3S$: C, 62.11; H, 2.76; S, 9.75; Found C, 62.14; H, 2.79; S, 9.65.

*5.3.32. 2-(benzo[b]thiophen-3-yl)-7-ethoxy-3-hydroxy-4H-chromen-4-one (**32**)*

Compound **32** was prepared according to the general method for the synthesis of flavonol-like compounds reported above starting from compound **58**. Compound **32** was isolated as a yellow solid in 25% yield. mp: 209–210 °C. ^{1}H NMR (400 MHz, DMSO) δ: 9.52 (s, 1H), 8.57 (s, 1H), 8.39 (d, J = 7.5 Hz, 1H), 8.12 (d, J = 7.5 Hz, 1H), 8.04 (d, J = 8.9 Hz, 1H), 7.57 - 7.48 (m, 2H), 7.26 (d, J = 2.3 Hz, 1H), 7.07 (dd, J = 8.9, 2.3 Hz, 1H), 4.22 (q, J = 7.0 Hz, 2H), 1.40 (t, J = 7.0 Hz, 3H). ^{13}C NMR (100 MHz, DMSO) δ: 171.81, 162.88, 156.21, 143.67, 139.08, 138.58, 136.40, 131.64, 126.17, 125.88, 125.11, 124.84, 124.47, 122.98, 115.45, 114.84, 100.66, 64.25, 14.36. ESI-HRMS calcd. for $C_{19}H_{15}O_4S$ $[M+H]^+$ 339.0686, found 339.0680. Anal. calcd. for $C_{19}H_{14}O_4S$: C, 67.44; H, 4.17; S, 9.47; Found C, 67.31; H, 4.13; S, 9.21.

*5.3.33. 2-(benzo[b]thiophen-3-yl)-6-methoxy-4-oxo-4H-chromen-3-yl acetate (**33**)*

Compound **33** was prepared according to the general method for the synthesis of ethers reported above starting from compound **19**. Compound **33** was isolated as a beige solid in 94% yield. mp: 180 °C dec. ^{1}H NMR (400 MHz, $CDCl_3$) δ: 8.16-8.12 (m, 1H), 8.07 (s, 1H), 7.97-7.93 (m, 1H), 7.66 (d, J = 3.1 Hz, 1H), 7.52 (d, J = 9.2 Hz, 1H), 7.52-7.46 (m, 2H), 7.34 (dd, J = 9.2, 3.1 Hz, 1H), 3.94 (s, 3H), 2.29 (s, 3H). ^{13}C NMR (100 MHz, $CDCl_3$) δ 170.70, 166.99, 156.12, 152.24, 149.40, 138.74, 135.49, 132.58, 130.42, 124.39, 124.25, 124.22, 123.51, 123.27, 122.82, 121.78, 118.43, 104.09, 54.99, 19.53. ESI-HRMS calcd. for $C_{20}H_{15}O_5S$ $[M+H]^+$ 367.0635, found 367.0631. Anal. calcd. for $C_{20}H_{14}O_5S$: C, 65.56; H, 3.85; S, 8.75; Found C, 65.40; H, 3.86; S, 8.61.

*5.3.34. 2-(benzo[b]thiophen-3-yl)-6-methoxy-4-oxo-4H-chromen-3-yl pivalate (**34**)*

Compound **34** was prepared according to the general method for the synthesis of ethers reported above starting from compound **19**. Compound **34** was isolated as a white solid in 93% yield. mp: 169 °C. ^{1}H NMR (400 MHz, $CDCl_3$) δ: 8.15-8.10 (m, 1H), 8.01 (s, 1H), 7.97-7.90 (m, 1H), 7.66 (d, J = 3.1 Hz, 1H), 7.51 (d, J = 9.1 Hz, 1H), 7.51-7.43 (m, 2H), 7.32 (dd, J = 9.2, 3.1 Hz, 1H), 3.91 (s, 3H), 1.30 (s, 9H). ^{13}C NMR (100 MHz, $CDCl_3$) δ 175.65, 171.72, 157.10, 153.13, 150.43, 139.69, 136.62, 133.89, 131.27, 125.37, 125.25, 125.21, 124.54, 124.25, 123.89, 122.78, 119.48, 104.96, 55.93, 39.07, 27.12. ESI-HRMS

calcd. for $C_{23}H_{21}O_5S$ $[M+H]^+$ 409.1104, found 409.1102. Anal. calcd. for $C_{23}H_{20}O_5S$: C, 67.63; H, 4.94; S, 7.85; Found C, 67.81; H, 5.05; S, 7.67.

*5.3.35. 2-(benzo[b]thiophen-3-yl)-6-methoxy-4-oxo-4H-chromen-3-yl pentanoate (**35**)*

Compound **35** was prepared according to the general method for the synthesis of ethers reported above starting from compound **19**. Compound **35** was isolated as a pale yellow solid in 53% yield. mp: 111–112 °C. ^{1}H NMR (400 MHz, $CDCl_3$) δ: 8.13-8.11 (m, 1H), 8.05 (s, 1H), 7.96-7.93 (m, 1H), 7.66 (d, $J = 3.1$ Hz, 1H), 7.51 (d, $J = 9.2$ Hz, 1H), 7.51-7.42 (m, 2H), 7.32 (dd, $J = 9.2$, 3.1 Hz, 1H), 3.92 (s, 3H), 2.55 (t, $J = 7.5$ Hz, 2H), 1.69-1.61 (m, 2H), 1.38-1.28 (m, 2H), 0.88 (t, $J = 7.4$ Hz, 3H). ^{13}C NMR (100 MHz, $CDCl_3$) δ: 171.79, 170.87, 157.12, 153.22, 150.44, 139.75, 136.56, 133.65, 131.39, 125.47, 125.25, 125.22, 124.55, 124.27, 123.88, 122.78, 119.46, 105.08, 55.99, 33.64, 26.88, 22.08, 13.67. ESI-HRMS calcd. for $C_{23}H_{21}O_5S$ $[M+H]^+$ 409.1104, found 409.1100. Anal. calcd. for $C_{23}H_{20}O_5S$: C, 67.63; H, 4.94; S, 7.85; Found C, 67.33; H, 4.83; S, 8.01.

*5.3.36. 2-(benzo[b]thiophen-3-yl)-6-methoxy-4-oxo-4H-chromen-3-yl dimethylcarbamate (**36**)*

Compound **36** was prepared according to the general method for the synthesis of carbamates reported above starting from compound **19**. Compound **36** was isolated as a yellow solid in 42% yield. mp: 221–222 °C. ^{1}H NMR (400 MHz, $CDCl_3$) δ: 8.18 (dd, $J = 7.2$, 1.5 Hz, 1H), 8.11 (s, 1H), 7.94 (dd, $J = 7.2$, 1.5 Hz, 1H), 7.66 (d, $J = 3.1$ Hz, 1H), 7.51 (d, $J = 9.1$ Hz, 1H), 7.51-7.43 (m, 2H), 7.32 (dd, $J = 9.1$, 3.1 Hz, 1H), 3.92 (s, 3H), 3.09 (s, 3H), 3.01 (s, 3H). ^{13}C NMR (100 MHz, $CDCl_3$) δ: 172.70, 156.98, 153.67, 153.40, 150.40, 139.78, 136.77, 134.33, 131.58, 125.54, 125.13, 125.11, 124.63, 124.10, 123.96, 122.76, 119.40, 105.08, 55.95, 37.07, 36.83. ESI-HRMS calcd. for $C_{21}H_{18}NO_5S$ $[M+H]^+$ 396.0900, found 396.0908. Anal. calcd. for $C_{21}H_{17}NO_5S$: C, 63.79; H, 4.33; N, 3.54; S, 8.11; Found C, 63.75; H, 4.58; N, 3.50; S, 7.90.

*5.3.37. 2-(benzo[b]thiophen-3-yl)-3-ethoxy-6-methoxy-4H-chromen-4-one (**37**)*

Compound **37** was prepared according to the general method for the synthesis of ethers reported above starting from compound **19**. Compound **37** was isolated as a yellow solid in 77% yield. mp: 146–147 °C. ^{1}H NMR (400 MHz, $CDCl_3$) δ: 8.46 (s, 1H), 8.31 (dd, $J = 7.4$, 0.9 Hz, 1H), 7.94 (dd, $J = 7.4$, 1.1 Hz, 1H), 7.66 (d, $J = 3.1$ Hz, 1H), 7.52 (d, $J = 9.1$ Hz, 1H), 7.51 (dd, $J = 7.0$, 1.2 Hz, 1H), 7.44 (dd, $J = 7.1$, 0.9 Hz, 1H), 7.30 (dd, $J = 9.1$, 3.1 Hz, 1H), 4.14 (q, $J = 7.0$ Hz, 2H), 3.94 (s, 3H), 1.27 (t, $J = 7.0$ Hz, 3H). ^{13}C NMR (100 MHz, $CDCl_3$) δ: 174.56, 156.79, 153.58, 149.91, 140.06, 139.68, 136.91, 132.31, 125.97, 125.04, 124.93, 124.32, 123.79, 122.79, 119.28, 104.73, 68.54, 55.97, 15.61. ESI-HRMS calcd. for $C_{20}H_{17}O_4S$ $[M+H]^+$ 353.0842, found 353.0845. Anal. calcd. for $C_{20}H_{16}O_4S$: C, 68.17; H, 4.58; S, 9.10; Found C, 67.92; H, 4.81; S, 9.11.

*5.3.38. 2-(benzo[b]thiophen-3-yl)-6-methoxy-3-propoxy-4H-chromen-4-one (**38**)*

Compound **38** was prepared according to the general method for the synthesis of ethers reported above starting from compound **19**. Compound **38** was isolated as an orange solid in 76% yield. mp: 137 °C. ^{1}H NMR (400 MHz, $CDCl_3$) δ: 8.33 (s, 1H), 8.20 (d, $J = 7.4$ Hz, 1H), 7.85 (d, $J = 7.4$, 1H), 7.57 (d, $J = 3.1$ Hz, 1H), 7.44-7.33 (m, 2H), 7.42 (d, $J = 9.2$ Hz, 1H), 7.21 (dd, $J = 9.1$, 3.1 Hz, 1H), 3.93 (t, $J = 6.7$ Hz, 2H), 3.85 (s, 3H), 1.66-1.50 (m, 2H), 0.77 (t, $J = 7.4$ Hz, 3H). ^{13}C NMR (100 MHz, $CDCl_3$) δ: 174.51, 156.78, 153.41, 149.92, 140.31, 139.66, 136.95, 132.25, 125.95, 125.06, 125.02, 124.92, 124.27, 123.76, 122.78, 119.28, 104.72, 74.56, 55.95, 23.35, 10.35. ESI-HRMS calcd. for $C_{21}H_{19}O_4S$ $[M+H]^+$ 367.0999, found 367.0998. Anal. calcd. for $C_{21}H_{18}O_4S$: C, 68.83; H, 4.95; S, 8.75; Found C, 69.18; H, 5.03; S, 8.53.

*5.3.39. (E)-3-(furan-2-yl)-1-(2-hydroxy-5-methoxyphenyl)prop-2-en-1-one (**39**)*

Compound **39** was prepared according to the general method for the synthesis of (2E)-1-(2-hydroxyphenyl)-3-phenylprop-2-en-1-ones reported above. Compound **39** was isolated as a red powder in 51% yield. mp: 73–74 °C. ^{1}H NMR ($CDCl_3$, 400 MHz) δ: 12.51 (br s, 1H), 7.71 (d, $J = 15.1$ Hz, 1H), 7.59 (d, $J = 1.8$ Hz, 1H), 7.52 (d, $J = 15.1$ Hz, 1H), 7.38 (d, $J = 3.0$ Hz, 1H), 7,17 (dd, $J = 9.1$, 3.0 Hz, 1H), 6.99 (d, $J = 9.1$ Hz, 1H), 6.81 (d, $J = 3.4$ Hz, 1H), 6.58 (dd, $J = 1.8$, 3.4 Hz, 1H), 3.87 (s, 3H). ^{13}C NMR ($CDCl_3$, 100 MHz) δ: 192.94, 157.99, 151.76, 151.54, 145.47, 131.25, 124.12, 119.64, 119.32, 117.60, 117.24, 112.95, 112.56, 56.12. MS (ESI) $m/z = 245.1$ $[M+H]^+$; 243.0 $[M-H]^-$.

*5.3.40. (E)-3-(furan-2-yl)-1-(2-hydroxy-4-methoxyphenyl)prop-2-en-1-one (**40**)*

Compound **40** was prepared according to the general method for the synthesis of (2E)-1-(2-hydroxyphenyl)-3-phenylprop-2-en-1-ones reported above. Compound **40** was isolated as an orange solid in 65% yield. mp: 118–120 °C. ^{1}H NMR ($CDCl_3$, 400 MHz) δ: 13.51 (br s, 1H), 7.83 (d, $J = 8.7$ Hz, 1H), 7.65 (d, $J = 15.1$ Hz, 1H), 7.55 (d, $J = 1.7$ Hz, 1H), 7.48 (d, $J = 15.1$ Hz, 1H), 6.74 (d, $J = 3.4$ Hz, 1H), 6.53 (dd, $J = 1.7$, 3.4 Hz, 1H), 6.49 (dd, $J = 8.7$, 2.5 Hz, 1H), 6.48 (d, 1H, $J = 2.5$ Hz, 1H), 3.86 (s, 3H). ^{13}C NMR ($CDCl_3$, 100 MHz) δ: 191.45, 166.61, 166.18, 151.66, 145.14, 131.24, 130.22, 117.90, 116.51, 114.15, 112.77, 107.68, 101.05, 55.57. MS (ESI) $m/z = 245.1$ $[M+H]^+$; 243.1 $[M-H]^-$.

*5.3.41. (E)-1-(2-hydroxy-5-methoxyphenyl)-3-(4-methylthiophen-2-yl)prop-2-en-1-one (**41**)*

Compound **41** was prepared according to the general method for the synthesis of (2E)-1-(2-hydroxyphenyl)-3-phenylprop-2-en-1-ones reported above. Compound **41** was isolated as an orange solid in 73% yield. mp: 79 °C. ^{1}H NMR ($CDCl_3$, 400 MHz) δ: 12.36 (br s, 1H), 8.00 (d, $J = 15.1$ Hz, 1H), 7.35 (d, $J = 15.1$ Hz, 1H), 7.33 (d, $J = 3.0$ Hz, 1H), 7.23 (m, 1H), 7,15 (dd, $J = 9.0$, 3.0 Hz, 1H), 7.08 (m, 1H), 6.98 (d, $J = 9.0$ Hz, 1H), 3.86 (s, 3H), 2.30 (d, $J = 0.7$ Hz, 3H). ^{13}C NMR ($CDCl_3$, 100 MHz) δ: 192.79, 157.88, 151.69, 139.82, 139.29, 138.20, 134.81, 125.36, 123.66, 119.63, 119.28, 118.36, 112.93, 56.16, 15.53. MS (ESI) $m/z = 275.1$ $[M+H]^+$.

*5.3.42. (E)-1-(2-hydroxy-4-methoxyphenyl)-3-(4-methylthiophen-2-yl)prop-2-en-1-one (**42**)*

Compound **42** was prepared according to the general method for the synthesis of (2E)-1-(2-hydroxyphenyl)-3-phenylprop-2-en-1-ones reported above. Compound **42** was isolated as a yellow solid in quantitative yield. mp 123–124 °C. ^{1}H NMR ($CDCl_3$, 400 MHz) δ ppm: 13.68 (br s, 1H), 7.94 (d, $J = 15.1$ Hz, 1H), 7.78 (d, $J = 8.7$ Hz, 1H), 7.31 (d, $J = 15.1$ Hz, 1H), 7.17 (s, 1H), 7.03 (s, 1H), 6.49 (dd, $J = 8.7$, 2.5 Hz, 1H), 3.86 (s, 3H), 2.32 (s, $J = 0.7$ Hz, 3H). ^{13}C NMR ($CDCl_3$, 100 MHz) δ: 191.29, 166.62, 166.15, 140.02, 139.15, 137.02, 134.35, 131.10, 124.85, 118.62, 114.04, 107.67, 101.06, 55.57, 15.53. MS (ESI) $m/z = 275.1$ $[M+H]^+$; 273.0 $[M-H]^-$.

*5.3.43. (E)-1-(2-hydroxy-5-methylphenyl)-3-(4-methylthiophen-2-yl)prop-2-en-1-one (**43**)*

Compound **43** was prepared according to the general method for the synthesis of (2E)-1-(2-hydroxyphenyl)-3-phenylprop-2-en-1-ones reported above. Compound **43** was isolated as an orange solid in 60% yield. mp: 104–105 °C. ^{1}H NMR (400 MHz, $CDCl_3$) δ: 12.71 (s, 1H), 7.99 (d, $J = 15.1$ Hz, 1H), 7.65 (d, $J = 1.6$ Hz, 1H), 7.41 (d, $J = 15.1$ Hz, 1H), 7.32 (dd, $J = 8.5$, 2.1 Hz, 1H), 7.23 (s, 1H), 7.07 (s, 1H), 6.94 (d, $J = 8.5$ Hz, 1H), 2.38 (s, 3H), 2.31 (d, $J = 0.7$ Hz, 3H). ^{13}C NMR (100 MHz, $CDCl_3$) δ: 193.07, 161.48, 139.92, 139.25, 137.85, 137.38,

134.66, 129.19, 127.88, 125.19, 119.63, 118.50, 118.32, 20.64, 15.54. MS (ESI) m/z = 259.1 $[M+H]^+$.

*5.3.44. (E)-1-(2-hydroxy-6-methoxyphenyl)-3-(4-methylthiophen-2-yl)prop-2-en-1-one (**44**)*

Compound **44** was prepared according to the general method for the synthesis of (2E)-1-(2-hydroxyphenyl)-3-phenylprop-2-en-1-ones reported above. Compound **44** was isolated as a yellow solid in quantitative yield. mp: 89 °C. ^{1}H NMR ($CDCl_3$, 400 MHz) δ: 13.11 (br s, 1H), 7.90 (d, J = 15.3 Hz, 1H), 7.68 (d, J = 15.3 Hz, 1H), 7.36 (t, J = 8.3 Hz, 1H), 7.15 (m, 1H), 7.00 (m, 1H), 6.62 (dd, J = 8.3, 0.8 Hz, 1H), 6.43 (d, J = 0.8 Hz, 1H), 3.95 (s, 3H), 2.28 (s, 3H). ^{13}C NMR ($CDCl_3$, 100 MHz) δ: 193.75, 164.90, 160.95, 140.71, 139.07, 135.91, 135.80, 133.90, 126.09, 124.38, 111.87, 110.90, 101.54, 55.89, 15.56. MS (ESI) m/z = 275.1 $[M+H]^+$; 273.0 $[M-H]^-$.

*5.3.45. (E)-1-(2-hydroxy-4-methoxyphenyl)-3-(3-methylthiophen-2-yl)prop-2-en-1-one (**45**)*

Compound **45** was prepared according to the general method for the synthesis of (2E)-1-(2-hydroxyphenyl)-3-phenylprop-2-en-1-ones reported above. Compound **45** was isolated as a yellow solid in 49% yield. mp: 128−129 °C. ^{1}H NMR ($CDCl_3$, 400 MHz) δ: 13.39 (br s, 1H), 8.12 (d, J = 15.0 Hz, 1H), 7.81 (d, J = 8.8 Hz, 1H), 7.35 (d, J = 5.1 Hz, 1H), 7.32 (d, J = 15.0 Hz, 1H), 6.94 (d, J = 5.1 Hz, 1H), 6.51 (dd, J = 8.8, 2.5 Hz, 1H), 6.49 (d, J = 2.5 Hz, 1H), 3.88 (s, 3H), 2.44 (s, 3H). ^{13}C NMR ($CDCl_3$, 100 MHz) δ: 191.39, 166.63, 166.12, 143.01, 135.28, 134.53, 131.53, 131.09, 127.68, 118.15, 114.07, 107.70, 101.06, 55.59, 14.33. MS (ESI) m/z = 275.1 $[M+H]^+$.

*5.3.46. (E)-1-(2-hydroxy-5-methylphenyl)-3-(5-methylthiophen-2-yl)prop-2-en-1-one (**46**)*

Compound **46** was prepared according to the general method for the synthesis of (2E)-1-(2-hydroxyphenyl)-3-phenylprop-2-en-1-ones reported above. Compound **46** was isolated as a light brown solid in 44% yield. mp: 113 °C. ^{1}H NMR (400 MHz, DMSO) δ: 12.24 (s, 1H), 8.01 (d, J = 15.1, 1H), 7.89-7.88 (m, 1H), 7.74 (d, J = 5.0 Hz, 1H), 7.54 (d, J = 15.1 Hz, 1H), 7.36 (dd, J = 8.4, 2.0 Hz, 1H), 7.06 (d, J = 5.0 Hz, 1H), 6.89 (d, J = 8.4 Hz, 1H), 2.39 (s, 3H), 2.31 (s, 3H). ^{13}C NMR (100 MHz, DMSO) δ: 192.38, 159.42, 143.64, 136.87, 135.24, 133.66, 131.74, 130.01, 129.58, 127.96, 120.54, 119.33, 117.48, 19.89, 13.95. MS (ESI) m/z = 259.1 $[M+H]^+$.

*5.3.47. (E)-3-(benzo[d] [1,3]dioxol-5-yl)-1-(2-hydroxy-4-methoxyphenyl)prop-2-en-1-one (**47**)*

Compound **47** was prepared according to the general method for the synthesis of (2E)-1-(2-hydroxyphenyl)-3-phenylprop-2-en-1-ones reported above. Compound **47** was isolated as a yellow solid in 44% yield. mp: 149 °C. ^{1}H NMR (400 MHz, $CDCl_3$) δ: 7.75-7.71 (m, 1H), 7.73 (d, J = 15.2 Hz, 1H), 7.45 (d, J = 15.2 Hz, 1H), 7.21 (d, J = 1.6 Hz, 1H), 7.18 (dd, J = 8.0, 1.6 Hz, 1H), 6.90 (d, J = 8.0 Hz, 1H), 6.52 (dd, J = 9.0, 2.5 Hz, 1H), 6.51 (s, 1H), 6.08 (s, 2H), 3.90 (s, 3H). ^{13}C NMR (100 MHz, $CDCl_3$) δ: 191.75, 166.66, 166.12, 150.06, 148.48, 144.25, 131.11, 129.30, 125.39, 118.30, 114.14, 108.72, 107.66, 106.72, 101.69, 101.10, 55.59. MS (ESI) m/z = 297.0 $[M+H]^+$.

*5.3.48. (E)-1-(2-hydroxy-5-methoxyphenyl)-3-(1H-indol-3-yl) prop-2-en-1-one (**48**)*

To a suspension of 2′-hydroxy-4′-methoxyacetophenone (1.00 g, 6.02 mmol) and 1H-indole-3-carbaldehyde (0.87 g, 6.02 mmol) in ethanol, piperidine (0.6 mL, 0.51 g, 6.02 mmol) was added. The reaction mixture was refluxed for 24 h. After the completion of the reaction, the mixture was cooled to 0 °C and neutralized with acetic acid. The resulting solid was collected by filtration, washed with ethanol and recrystallized from ethanol to give compound **48** as an orange solid in 54% yield. mp 206 °C. ^{1}H NMR (400 MHz, DMSO) δ: 12.48 (br s, 1H), 12.04 (br s, 1H), 8.24 (s, 1H), 8.19 (d, J = 15.3 Hz, 1H), 8.11 - 8.07 (m, 1H), 7.76 (d, J = 15.3 Hz, 1H), 7.61 (d, J = 3.0 Hz, 1H), 7.54 - 7.50 (m, 1H), 7.29 - 7.23 (m, 2H), 7.19 (dd, J = 9.0, 3.0 Hz, 1H), 6.94 (d, J = 9.0 Hz, 1H), 3.83 (s, 3H). ^{13}C NMR (100 MHz, DMSO) δ: 193.03, 156.37, 152.03, 140.44, 137.96, 134.24, 125.78, 123.33, 123.16, 121.85, 121.27, 120.67, 118.98, 115.21, 113.75, 113.42, 113.00, 56.29. MS (ESI) m/z = 292.0 $[M-H]^-$.

*5.3.49. (E)-3-(benzo[b]thiophen-3-yl)-1-(2-hydroxy-5-methylphenyl)prop-2-en-1-one (**49**)*

Compound **49** was prepared according to the general method for the synthesis of (2E)-1-(2-hydroxyphenyl)-3-phenylprop-2-en-1-ones reported above. Compound **49** was isolated as an orange solid in 55% yield. mp: 139 °C. ^{1}H NMR (400 MHz, $CDCl_3$) δ: 12.71 (s, 1H), 8.23 (d, J = 15.5 Hz, 1H), 8.13 (d, J = 8.1 Hz, 1H), 7.99 (s, 1H), 7.94 (d, J = 8.1 Hz, 1H), 7.77 (d, J = 15.5 Hz, 1H), 7.72 (d, J = 1.5 Hz, 1H), 7.57 - 7.53 (m, 1H), 7.49-7.45 (m, 1H), 7.36 (dd, J = 8.5, 1.5 Hz, 1H), 6.98 (d, J = 8.5 Hz, 1H), 2.39 (s, 3H). ^{13}C NMR (100 MHz, $CDCl_3$) δ:193.50, 161.58, 140.57, 137.52, 137.34, 136.65, 132.27, 129.26, 129.15, 127.96, 125.28, 125.19, 123.13, 122.14, 120.72, 119.69, 118.45, 20.67. MS (ESI) m/z = 295.1 $[M+H]^+$.

*5.3.50. (E)-3-(benzo[b]thiophen-3-yl)-1-(5-bromo-2-hydroxyphenyl)prop-2-en-1-one (**50**)*

Compound **50** was prepared according to the general method for the synthesis of (2E)-1-(2-hydroxyphenyl)-3-phenylprop-2-en-1-ones reported above. Compound **50** was isolated as an orange solid in 74% yield. mp: 159 °C. ^{1}H NMR (400 MHz, $CDCl_3$) δ: 12.83 (s, 1H), 8.25 (d, J = 15.4 Hz, 1H), 8.11 (d, J = 8.0 Hz, 1H), 8.02 (s, 1H), 8.02 (d, J = 2.4 Hz, 1H), 7.94 (dd, J = 8.0, 0.8 Hz, 1H), 7.65 (d, J = 15.4 Hz, 1H), 7.60 (dd, J = 8.9, 2.4 Hz, 1H), 7.58-7.53 (m, 1H), 7.50-7.46 (m, 1H), 6.97 (d, J = 8.9 Hz, 1H). ^{13}C NMR (100 MHz, $CDCl_3$) δ: 192.56, 162.54, 140.54, 138.95, 137.81, 137.21, 131.95, 131.75, 130.04, 125.40, 125.34, 123.17, 122.08, 121.27, 120.70, 119.67, 110.49. MS (ESI) m/z ^{79}Br = 359.1 $[M+H]^+$; ^{81}Br = 361.1 $[M+H]^+$.

*5.3.51. (E)-3-(benzo[b]thiophen-3-yl)-1-(5-fluoro-2-hydroxyphenyl)prop-2-en-1-one (**51**)*

Compound **51** was prepared according to the general method for the synthesis of (2E)-1-(2-hydroxyphenyl)-3-phenylprop-2-en-1-ones reported above. Compound **51** was isolated as an orange solid in 55% yield. mp: 168 °C. ^{1}H NMR (400 MHz, $CDCl_3$) δ: 12.62 (s, 1H), 8.26 (dd, J = 15.4, 0.7 Hz, 1H), 8.12 (d, J = 7.9 Hz, 1H), 8.01 (s, 1H), 7.96-7.93 (m, 1H), 7.65 (d, J = 15.5 Hz, 1H), 7.61 (dd, J = 9.1, 3.1 Hz, 1H), 7.56 (ddd, J = 8.2, 7.1, 1.2 Hz, 1H), 7.51-7.46 (m, 1H), 7.31-7.26 (m, 1H), 7.04 (dd, J = 9.1, 4.6 Hz, 1H). ^{13}C NMR (100 MHz, $CDCl_3$) δ: 192.72 (d, J = 2.7 Hz), 159.80 (d, J = 1.2 Hz), 154.90 (d, J = 238.3 Hz), 140.60, 137.77, 137.15, 132.01, 130.17, 125.40, 125.34, 123.92 (d, J = 23.6 Hz), 123.19, 122.13, 119.93 (d, J = 7.3 Hz), 119.76, 119.52 (d, J = 6.1 Hz), 114.45 (d, J = 23.3 Hz). MS (ESI) m/z = 299.2 $[M+H]^+$.

*5.3.52. (E)-3-(benzo[b]thiophen-3-yl)-1-(5-chloro-2-hydroxyphenyl)prop-2-en-1-one (**52**)*

Compound **52** was prepared according to the general method for the synthesis of (2E)-1-(2-hydroxyphenyl)-3-phenylprop-2-en-1-ones reported above. Compound **52** was isolated as an orange solid in 76% yield. mp: 163−164 °C. ^{1}H NMR (400 MHz, $CDCl_3$) δ: 12.78 (s, 1H), 8.25 (d, J = 15.4 Hz, 1H), 8.10 (d, J = 8.0 Hz, 1H), 8.02 (s, 1H), 7.93 (d, J = 8.0 Hz, 1H), 7.88 (d, J = 2.5 Hz, 1H), 7.66 (d, J = 15.4 Hz, 1H), 7.54 (ddd, J = 8.1, 7.1, 1.1 Hz, 1H), 7.49-7.43 (m, 2H), 7.01 (d, J = 8.9 Hz, 1H). ^{13}C NMR (100 MHz, $CDCl_3$) δ: 192.67, 162.11, 140.57, 137.86, 137.20, 136.21, 131.98, 130.12, 128.74, 125.41, 125.35, 123.58, 123.19, 122.11, 120.62, 120.31, 119.70. MS (ESI) m/z ^{35}Cl = 315.0 $[M+H]^+$; ^{37}Cl = 317.0 $[M+H]^+$.

*5.3.53. (E)-3-(benzo[b]thiophen-3-yl)-1-(2-hydroxyphenyl)prop-2-en-1-one (**53**)*

Compound **53** was prepared according to the general method for the synthesis of (2E)-1-(2-hydroxyphenyl)-3-phenylprop-2-en-1-ones reported above. Compound **53** was isolated as a yellow solid in 58% yield. mp: 140 °C. ^{1}H NMR (400 MHz, $CDCl_3$) δ: 12.93 (s, 1H), 8.22 (d, J = 15.5 Hz, 1H), 8.11 (d, J = 7.9 Hz, 1H), 7.96-7.91 (m, 3H), 7.75 (d, J = 15.5 Hz, 1H), 7.55-7.51 (m, 2H), 7.48-7.44 (m, 1H), 7.08 (dd, J = 8.4, 1.1 Hz, 1H), 6.99 (ddd, J = 8.2, 7.2, 1.1 Hz, 1H). ^{13}C NMR (100 MHz, $CDCl_3$) δ: 193.57, 163.66, 140.59, 137.24, 136.91, 136.42, 132.19, 129.59 (2C), 125.31, 125.23, 123.16, 122.17, 120.37, 120.04, 118.92, 118.70. MS (ESI) m/z = 281.1 $[M+H]^+$.

*5.3.54. (E)-3-(benzo[b]thiophen-3-yl)-1-(2-hydroxy-4-methoxyphenyl)prop-2-en-1-one (**54**)*

Compound **54** was prepared according to the general method for the synthesis of (2E)-1-(2-hydroxyphenyl)-3-phenylprop-2-en-1-ones reported above. Compound **54** was isolated as a yellow solid in 69% yield. mp 215 °C. ^{1}H NMR (400 MHz, $CDCl_3$) δ: 13.51 (s, 1H), 8.20 (d, J = 15.5 Hz, 1H), 8.12 (d, J = 7.9 Hz, 1H), 7.97-7.91 (m, 2H), 7.86 (d, J = 8.7 Hz, 1H), 7.69 (d, J = 15.5 Hz, 1H), 7.55-7.51 (m, 1H), 7.48-7.44 (m, 1H), 6.55-6.51 (m, 2H), 3.89 (s, 3H). ^{13}C NMR (100 MHz, $CDCl_3$) δ: 191.70, 166.76, 166.27, 140.59, 137.31, 135.95, 132.34, 131.17, 128.94, 125.23, 125.14, 123.12, 122.19, 120.73, 114.10, 107.84, 101.13, 55.63. MS (ESI) m/z = 311.1 $[M+H]^+$.

*5.3.55. (E)-3-(benzo[b]thiophen-3-yl)-1-(2-hydroxy-4-methylphenyl)prop-2-en-1-one (**55**)*

Compound **55** was prepared according to the general method for the synthesis of (2E)-1-(2-hydroxyphenyl)-3-phenylprop-2-en-1-ones reported above. Compound **55** was isolated as an orange solid in 58% yield. mp: 146 °C. ^{1}H NMR (400 MHz, $CDCl_3$) δ: 12.94 (s, 1H), 8.19 (d, J = 15.5 Hz, 1H), 8.10 (d, J = 8.1 Hz, 1H), 7.93 (s, 1H), 7.91 (d, J = 8.1 Hz, 1H), 7.81 (d, J = 8.2 Hz, 1H), 7.72 (d, J = 15.5 Hz, 1H), 7.53-7.49 (m, 1H), 7.47-7.41 (m, 1H), 6.85 (s, 1H), 6.77 (dd, J = 8.2, 1.2 Hz, 1H), 2.38 (s, 3H). ^{13}C NMR (100 MHz, $CDCl_3$) δ: 192.97, 163.83, 148.15, 140.59, 137.29, 136.45, 132.28, 129.45, 129.20, 125.26, 125.18, 123.13, 122.18, 120.64, 120.24, 118.74, 117.84, 22.04. MS (ESI) m/z = 295.1 $[M+H]^+$.

*5.3.56. (E)-3-(benzo[b]thiophen-3-yl)-1-(4-fluoro-2-hydroxyphenyl)prop-2-en-1-one (**56**)*

Compound **56** was prepared according to the general method for the synthesis of (2E)-1-(2-hydroxyphenyl)-3-phenylprop-2-en-1-ones reported above. Compound **56** was isolated as an orange solid in 58% yield. mp: 172–173 °C. ^{1}H NMR (400 MHz, $CDCl_3$) δ: 13.18 (d, J = 1.4 Hz, 1H), 8.14 (dd, J = 15.4, 0.7 Hz, 1H), 8.03 - 8.00 (m, 1H), 7.88-7.85 (m, 2H), 7.84-7.82 (m, 1H), 7.58 (d, J = 15.5 Hz, 1H), 7.44 (ddd, J = 8.2, 7.1, 1.2 Hz, 1H), 7.41-7.34 (m, 1H), 6.65 (dd, J = 10.4, 2.5 Hz, 1H), 6.60 (ddd, J = 8.9, 8.1, 2.5 Hz, 1H). ^{13}C NMR (100 MHz, $CDCl_3$) δ: 192.42, 167.48 (d, J = 257.0 Hz), 166.24 (d, J = 14.3 Hz), 140.60, 137.20, 137.19, 132.10, 131.86 (d, J = 11.9 Hz), 129.75, 125.35, 125.27, 123.18, 122.13, 120.16, 117.09 (d, J = 2.2 Hz), 107.19 (d, J = 22.8 Hz), 105.23 (d, J = 23.5 Hz). MS (ESI) m/z = 299.1 $[M+H]^+$.

*5.3.57. (E)-3-(benzo[b]thiophen-3-yl)-1-(4-chloro-2-hydroxyphenyl)prop-2-en-1-one (**57**)*

Compound **57** was prepared according to the general method for the synthesis of (2E)-1-(2-hydroxyphenyl)-3-phenylprop-2-en-1-ones reported above. Compound **57** was isolated as a yellow solid in 59% yield. mp: 194 °C. ^{1}H NMR (400 MHz, DMSO) δ: 12.59 (s, 1H), 8.68 (s, 1H), 8.24 (d, J = 7.6 Hz, 1H), 8.19 (d, J = 8.6 Hz, 1H), 8.13 (d, J = 15.6 Hz, 1H), 8.11 (dd, J = 7.2, 0.8 Hz, 1H), 8.04 (d, J = 15.6 Hz, 1H), 7.59 - 7.53 (m, 1H), 7.51 - 7.47 (m, 1H), 7.13 (d, J = 2.1 Hz, 1H), 7.09 (dd, J = 8.6, 2.1 Hz, 1H). ^{13}C NMR (100 MHz, DMSO) δ: 192.26, 161.91, 139.91, 139.90, 136.88, 135.95, 132.33, 131.99, 131.44, 125.32, 125.24, 123.37, 122.43, 122.15, 120.52, 119.49, 117.36. MS (ESI) m/z ^{35}Cl = 315.0 $[M+H]^+$; ^{37}Cl = 317.0 $[M+H]^+$.

*5.3.58. (E)-3-(benzo[b]thiophen-3-yl)-1-(4-ethoxy-2-hydroxyphenyl)prop-2-en-1-one (**58**)*

Compound **58** was prepared according to the general method for the synthesis of (2E)-1-(2-hydroxyphenyl)-3-phenylprop-2-en-1-ones reported above. Compound **58** was isolated as a yellow solid in 52% yield. mp: 152 °C. ^{1}H NMR (400 MHz, $CDCl_3$) δ: 13.49 (s, 1H), 8.20 (d, J = 15.5 Hz, 1H), 8.13 (d, J = 7.9 Hz, 1H), 7.96-7.92 (m, 2H), 7.86 (d, J = 8.9 Hz, 1H), 7.70 (d, J = 15.5 Hz, 1H), 7.54 (ddd, J = 8.2, 7.1, 1.2 Hz, 1H), 7.49-7.45 (m, 1H), 6.52 (dd, J = 8.9, 2.5 Hz, 1H), 6.50 (d, J = 2.5 Hz, 1H), 4.13 (q, J = 7.0 Hz, 2H), 1.47 (t, J = 7.0 Hz, 3H). ^{13}C NMR (100 MHz, $CDCl_3$) δ: 191.65, 166.75, 165.70, 140.59, 137.32, 135.87, 132.37, 131.15, 128.87, 125.22, 125.14, 123.12, 122.20, 120.80, 113.97, 108.20, 101.55, 63.99, 14.57. MS (ESI) m/z = 325.2 $[M+H]^+$.

*5.3.59. 3′,4′-dimethoxy-[1,1′-biphenyl]-3-carbaldehyde (**59**)*

The intermediate **59** was prepared according to the general method for the synthesis of biaryl aldehydes reported above. Compound **59** was isolated in 62% yield. ^{1}H NMR (200 MHz, $CDCl_3$) δ: 10.10 (s, 1H), 8.09-8.07 (m, 1H), 7.87-7.81 (m, 2H), 7.60 (t, J = 7.6 Hz, 1H), 7.21 (dd, J = 8.2, 2.0 Hz, 1H), 7.15 (d, J = 2.0 Hz, 1H), 6.99 (d, J = 8.2 Hz, 1H), 3.98 (s, 3H), 3.95 (s, 3H).

*5.3.60. 3-(benzo[d] [1,3]dioxol-5-yl)benzaldehyde (**60**)*

The intermediate **60** was prepared according to the general method for the synthesis of biaryl aldehydes reported above. Compound **60** was isolated in 54% yield. ^{1}H NMR (200 MHz, $CDCl_3$) δ: 10.07 (s, 1H), 8.04-8.02 (m, 1H), 7.85-7.75 (m, 2H), 7.59 (d, J = 7.6 Hz, 1H), 7.13-7.07 (m, 2H), 6.91 (d, J = 8.5 Hz, 1H), 6.02 (s, 2H).

5.4. General bioassay procedures

5.4.1. In vitro evaluation of activity against L. infantum intra macrophage amastigotes

The efficacy of compounds **1**–**13** against *L. infantum* intracellular amastigotes at 10 μM was determined according to the literature [16,43].

5.4.2. In vitro evaluation of activity against L. donovani and L. major

Infections of bone marrow-derived macrophages and parasite load quantification was performed as described in literature [16].

5.4.3. In vitro evaluation of activity against T. brucei

The efficacy of compounds against *T. brucei* bloodstream forms was evaluated using a modified resazurin-based assay previously described in literature [16]. The results are reported as the EC_{50} from the arithmetic average of at least two independent determinations performed in triplicate.

5.4.4. In vitro evaluation of activity against T. cruzi

Infections were performed in 6-well plates (3×10^6 HG39 cells/well). Confluent HG39 cells were infected with trypomastigotes of *T. cruzi* Y strain at a 1:1 ratio. The method used to assess the growth inhibition effect is based on the LGC Genomics, Berlin kit for the gDNAs detection. TaqMan™ probe-based quantitative real-time PCR was performed.

The assay against a *T. cruzi* panel of strains was performed as previously described [44]. Activity values were processed with the Graphpad Prism software (version 7), for generation of sigmoidal dose-response (variable slope) non-linear curve fitting and determination of EC_{50} values by interpolation. The assay was performed

in duplicate.

5.4.5. Cytotoxicity assessment against THP-1 macrophages

The effect of compounds **1**-**13** on THP-1-derived macrophages was assessed by the colorimetric MTT assay with (3-(4,5-dimethylthiazol-2-yl)-2,5-diphenyl tetrazolium bromide. The results are reported as the CC_{50} and NOAEL from the arithmetic average of at least two independent determinations performed in duplicate.

5.4.6. Early ADME-Toxicity assays

These made use of the *h*ERG Predictor™ Fluorescence Polarisation Assay (Invitrogen), P450-Glo™ Cytochrome P450 1A2, 2C9, 2C19, 2D6 and 3A4 Assays (Promega), CellTiter-Glo® Luminescent Cell Viability Assay (Promega) in the A549 and WI38 cell-lines and MitoTracker® Red chloromethyl-Xrosamine (CMXRos) uptake and High Content Imaging for assessment of mitochondrial toxicity as described in literature [45].

*5.4.7. Analytical procedure for miltefosine and compound **19***

Compound **19** and miltefosine were quantified using Liquid Chromatography-Mass Spectrometry (LC-MS) with a Gemini C18, 150 mm × 2.0 mm I.D., 5 μm particle size column (Phenomenex 00G-4435-B0). Briefly, plasma samples were mixed 0.5 mL acetonitrile to precipitate proteins. Samples were vortexed and then centrifuged at 4,020*g* for 15 min, filtered (0.45 μm mesh) (PTFE, VWR) and assayed. Chromatographic separation was carried out using a Shimadzu liquid cromatograph system consisting of two pumps, column oven, degasser and autosampler. The HPLC system was connected to a triple-quadrupole mass spectrometer equipped with a turboionspray source operated with unit resolution in the positive ion mode (ESI-QQQMS, Shimadzu LCMS-30) at the "CAI Espectrometría de Masas", Complutense University of Madrid (Spain). Plasma samples from mice were used as blank samples for snapshot studies. Calibration standards were freshly prepared before each analytical run with acetonitrile and purified water (25, 50, 100, 250, 500 and 1000 ng/mL). The lowest limit of quantification (LLOQ) was 17.6 ng/mL and the lowest limit of detection (LLOD) was 5.15 ng/mL All procedures were carried out at r.t.

*5.4.8. Snapshot of compound **19***

The pharmacological characteristics of compound **19** were evaluated by the snapshot method [46]. Compound **19** was dispersed in saline isotonic solution plus DMSO (8% v/v) and administered at 1 mg Kg^{-1} (IV) and at 20 mg Kg^{-1} (PO). For IV administration, 0.1 mL of the solution was administered to BALB/c mice (Harlan Laboratories, Barcelona, Spain) by injection in the tail vein. The volume for PO of compound **19** was 0.2 mL and given to mice using a 22G feeding needle. Blood samples were taken from facial vein at 0, 15, 30, 45 and 60 min and then at 3, 24, 48 and 72 h. Additional sample at 5 min was included from IV administered animals. Plasma was obtained and analyzed immediately or stored at −20 °C until analysis.

*5.4.9. Evaluation of efficacy of compound **19** in hamsters*

Male Syrian hamsters were obtained from Janvier Labs (France). When the hamsters reached *ca.* 120 g they were IV infected with 10^8 promastigotes of *L. infantum* (BCN150) and infection was allowed to progress for 15 weeks. CDs formulations were prepared by dispersing compound **19** in hydroxypropyl-β-cyclodextrin (Cavasol© W7 HP Pharma, Ashland, Switzerland) up to final concentrations of 30% v/v or 50% v/v CDs v/v in saline isotonic solution. Infected animals were divided in a weight stratified way into 7 groups. Groups 13–15 (G13-G15), 6 animals each, were the infected control groups receiving the vehicles (G13: DMSO 8% v/v; G14: 30% v/v CDs; G15: 50% v/v CDs). G16 (7 animals) was treated with free compound **19** formulated with DMSO 8%; G17 (7 animals) received the compound **19** with 30% v/v CDs; G18 (n = 7) was treated with compound **19** with 50% v/v CDs. Compound **19** was administered at the dose of 40 mg/kg/day (20 mg/kg, every 12 h), for 10 days. Infected groups G13-G15 received equal volume and followed the same treatment schedule of vehicles solution than treated groups. G20 (8 hamsters) was treated with miltefosine (Sigma) (20 mg/kg/day, 10 days). All treatments were administered PO with 20G feeding needle. In addition an uninfected and untreated control group of six animals was included in the experiment (G12). During the experiments, animals were observed daily and weighed weekly; blood samples were taken every 15 days and clinical signs and lesions recorded. Ten to sixteen days after the last treatment, the animals were euthanatized by isoflurane overdose, bled by intracardiac puncture and dissected.

*5.4.10. Toxicity of compound **19** and efficacy criteria in hamsters*

Clinical course and lesions during the experimental infection and treatment were recorded. In addition, immediate adverse effects after medication were annotated. Liver and spleen markers (AST, ALT, AP, Creatinine and urea) were determined at the end of the experiment. All animals, after euthanasia, were dissected and the weight and gross pathology of major target visceral organs, spleen and liver, were examined. Samples from both organs were taken and the leishmanial burden determined (Leishman Donovan Units, LDU) on spleen and liver smears stained with May-Grünwald Giemsa. Amastigotes/500 host cell nuclei were determined and efficacy was expressed as the reduction observed in the treated animal groups compared to the infected and untreated control hamsters.

5.4.11. Serum antibody response in hamsters

Enzyme-Linked Immunosorbent Assay (ELISA) was performed to monitor *Leishmania*-specific IgG antibodies in peripheral blood of uninfected control and infected animals. Soluble antigen (40 μg/mL) of promastigotes cultures were used for coating Maxisorp® 96-well plates (Nunc) 50 μL/well at 4 °C overnight. PBS-BSA 2% w/v (75 μL/well) was employed to block the plates for 1 h at 37 °C. Sera samples taken at different time points were added 50 μL/well at a 1/50 dilution and incubated at for 2 h at 37 °C. Goat anti-hamster IgG (H + L)-HRP (Southern Biotech) was used as secondary antibody (50 μL/well), 1/2000 diluted and incubated for 30 min at r.t. Two to five washes with PBS-Tween 20 (0.05% v/v) were included between steps [47]. O-phenylenediamine (1 mg/mL) (Sigma) plus H_2O_2 (1/1000) solution was added 100 μL/well as HRP-enzyme substrate and the reaction was stop with H_2SO_4 (3 N) 50μL/well.

5.4.12. Resistance studies

L. donovani strains 1SR, BPK091 and BPK190 were cultivated in supplemented Medium 199. Selection of strain 1SR was performed by seeding promastigotes at 1×10^5 cells/mL into medium supplemented with solvent (DMSO) or empirically determined EC_{50} of each compound. Cell density was determined daily using a Schärfe System CASY cell counter. After 3 days, cells were diluted into fresh drug- or solvent-supplemented medium at 1×10^5 cells/mL. This procedure was repeated 11 times. A genomic DNA cosmid library was prepared from the DNA of *L. donovani* strain BPK190 as described before [27]. The cosmid DNA was prepared from that library and used to electrotransfect *L. donovani* BPK091 promastigotes as described [27]. Using Cos-Seq DNA analysis [28,29]>90% genome sequence coverage of the cosmid library in the recombinant parasites was ascertained, and the recombinant population was subjected to the drug/lead selection scheme outlined above. Cosmids isolated from the selected populations were subjected to

NGS on an Illumina MiSeq system and the obtained reads were aligned to the *L. infantum* genome (TriTrypDB-41_LinfantumJPCM5_Genome.fasta)using the Bowtie2 algorithm within the Assemble module of the MacVector™ software suite (versio 12.x).

5.4.13. UV–visible and fluorescence investigation

The one-photon absorption spectra were measured with a Cary 100 UV–visible spectrophotometer using 1 cm quartz cuvettes. The steady-state fluorescence spectra were obtained on a Spex Jobin-Yvon FluoroMax3 spectrofluorometer and were corrected for the spectral sensitivity of the excitation and the emission channels. The time-resolved emission measurements were performed with a Horiba FluoroMax4 time-correlated single-photon counting equipment using a 340 nm emitting 1.3 ns laser diode. To obtain a lifetime profile, each emission decay was described as the sum of 3 or 4 exponentials, each characterized by a pre-exponential factor and a decay constant, the reciprocal of the lifetime. A least-squares deconvolution procedure, based on the classical Marquardt algorithm, was employed (DAS-6 Horiba software). The estimated time resolution after deconvolution is 200 ps HSA (Sigma, ≥97% purity), BSA (Sigma, ≥ 99% purity), pepsin from porcine gastric mucosa (Sigma, 3200–4500 units/mg), trypsin from bovine pancreas (Sigma, ≥6,000 BAEE units/mg) and β-casein from bovine milk (Sigma, ≥ 98% purity) were used as such.

5.4.14. Ethics Statement

The experimental design and housing conditions at UCM were approved by the Committee of Animal Experimentation (Universidad Complutense de Madrid) and regional authorities (Community of Madrid) (Ref. PROEX 169/15). Experiments were carried out at the animal house with official identification code ES280790001164 following the 3Rs principles. Animal handling and sampling were performed by trained and officially qualified personnel.

Acknowledgements

This project has received funding from the European Union's Seventh Framework Programme for research, technological development and demonstration under grant agreement n° 603240 (NMTrypI - New Medicines for Trypanosomatidic Infections, https://fp7-nmtrypi.eu). The authors would like to thank the help with the animal experiments from Montserrat Grau DVM from the Instituto de Investigación Hospital 12 de Octubre (Madrid). The authors acknowledge the COST Action CM1307, http://www.cost.eu/COST_Actions/cmst/CM1307 for the contribution to the discussion of the research results and for providing the Short Term Fellowship (STSM) to perform the experiments on compounds fluorescence.

Appendix A. Supplementary data

Supplementary data to this article can be found online at https://doi.org/10.1016/j.ejmech.2019.111676.

Abbreviations

WHO	World Health Organization
NTDs	Neglected Tropical diseases
HAT	Human African trypanosomiasis
DNDi	Drugs for Neglected Diseases initiative
L. infantum	*Leishmania infantum*
L. donovani	*Leishmania donovani*
L. major	*Leishmania major*
T. brucei	*Trypanosoma brucei*
T. cruzi	*Trypanosoma cruzi*
$CDCl_3$	deuterated trichloromethane
EtOH	Ethanol
MeOH	Methanol
NaOH	sodium hydroxide
TMS	Trimethylsilane
IV	intravenous
PBS	phosphate-buffered saline
ACN	acetonitrile
EC_{50}	half maximal effective concentration
CC_{50}	half maximal cytotoxicity concentration
THP1	human monocytic cell line
A549	human lung adenocarcinoma epithelial cell line;
HSA	human serum albumin
BSA	bovine serum albumin
MIL	Miltefosine.

References

[1] M.N. Soeiro, K. Werbovetz, D.W. Boykin, W.D. Wilson, M.Z. Wang, A. Hemphill, Novel amidines and analogues as promising agents against intracellular parasites: a systematic review, Parasitology 140 (2013) 929–951.
[2] S.M. Teixeira, R.M. de Paiva, M.M. Kangussu-Marcolino, W.D. Darocha, Trypanosomatid comparative genomics: Contributions to the study of parasite biology and different parasitic diseases, Genet. Mol. Biol. 35 (2012) 1–17.
[3] G. Eperon, M. Balasegaram, J. Potet, C. Mowbray, O. Valverde, F. Chappuis, Treatment options for second-stage gambiense human African Trypanosomiasis, Expert Rev. Anti Infect. Ther. 12 (2014) 1407–1417.
[4] S.L. Croft, S. Sundar, A.H. Fairlamb, Drug resistance in leishmaniasis, Clin. Microbiol. Rev. 19 (2006) 111–126.
[5] K. Seifert, F.J. Pérez-Victoria, M. Stettler, M.P. Sánchez-Cañete, S. Castanys, F. Gamarro, S.L. Croft, Inactivation of the miltefosine transporter, LdMT, causes Miltefosine resistance that is conferred to the amastigote stage of Leishmania donovani and persists in vivo, Int. J. Antimicrob. Agents 3 (2007) 229–235.
[6] H.C. Maltezou, Drug resistance in visceral leishmaniasis, J. Biomed. Biotechnol. 2010 (2010) 617521.
[7] C. Schäfer, P. Tejera Nevado, D. Zander, J. Clos, ARM58 overexpression reduces intracellular antimony concentration in Leishmania infantum, Antimicrob. Agents Chemother. 58 (2014) 1565–1574.
[8] M. Yasinzai, M. Khan, A. Nadhman, G. Shahnaz, Drug resistance in leishmaniasis: current drug-delivery systems and future perspectives, Future Med. Chem. 5 (2013) 1877–1888.
[9] M. Reddy, S.S. Gill, S.R. Kalkar, W. Wu, P.J. Anderson, P.A. Rochon, Oral drug therapy for multiple neglected tropical diseases: a systematic review, J. Am. Med. Assoc. 298 (2007) 1911–1924.
[10] I.H. Gilbert, Drug discovery for neglected diseases: molecular target-based and phenotypic approaches, J. Med. Chem. 56 (2013) 7719–7726.
[11] M.L. Sykes, V.M. Avery, Approaches to protozoan drug discovery: phenotypic screening, J. Med. Chem. 56 (2013) 7727–7740.
[12] E. Uliassi, L. Piazzi, F. Belluti, A. Mazzanti, M. Kaiser, R. Brun, C.B. Moraes, L.H. Freitas-Junior, S. Gul, M. Kuzikov, B. Ellinger, C. Borsari, M.P. Costi, M.L. Bolognesi, Development of a focused library of triazole-linked privileged-structure-based conjugates leading to the discovery of novel phenotypic hits against Protozoan parasitic infections, ChemMedChem 13 (2018) 678–683.
[13] D. Tasdemir, M. Kaiser, R. Brun, V. Yardley, T.J. Schmidt, F. Tosun, P. Rüedi, Antitrypanosomal and antileishmanial activities of flavonoids and their analogues: in vitro, in vivo, structure-activity relationship, and quantitative structure-activity relationship studies, Antimicrob. Agents Chemother. 50 (2006) 1352–1364.
[14] E.R. da Silva, C. MaquiaveliCdo, P.P. Magalhães, The leishmanicidal flavonols quercetin and quercitrin target Leishmania (Leishmania) amazonensis arginase, Exp. Parasitol. 130 (2012) 183–188.
[15] S. Arioka, M. Sakagami, R. Uematsu, H. Yamaguchi, H. Togame, H. Takemoto, H. Hinou, S. Nishimura, Potent inhibitor scaffold against Trypanosoma cruzi trans-sialidase, Bioorg. Med. Chem. 18 (2010) 1633–1640.
[16] C. Borsari, R. Luciani, C. Pozzi, I. Pöhner, S. Henrich, M. Trande, A. Cordeiro-da-Silva, N. Santarém, C. Baptista, A. Tait, F. Di Pisa, L. Dello Iacono, G. Landi, S. Gul, M. Wolf, M. Kuzikov, B. Ellinger, J. Reinshagen, G. Witt, P. Gribbon, M. Kohler, O. Keminer, B. Behrens, L. Costantino, P. TejeraNevado, E. Bifeld, J. Eick, J. Clos, J. Torrado, M.D. Jiménez-Antón, M.J. Corral, J.M. Alunda, F. Pellati, R.C. Wade, S. Ferrari, S. Mangani, M.P. Costi, Profiling of flavonol derivatives for the development of anti-trypanosomatidic drugs, J. Med. Chem. 59 (2016) 7598–7616.
[17] M.P. Costi, L. Costantino, C. Borsari, S. Ferrari, J.M. Alunda Rodriguez, A. Cordeiro-da-Silva, Nuove Molecole Ad Attivita' Antiparassitaria, Italian Patent: 102017000028966.
[18] L.H. Cazarolli1, L. Zanatta, E.H. Alberton, M. Santos Reis Bonorino Figueiredo, P. Folador, R. Guollo Damazio, M.G. Pizzolatti, F.R. Mena Barreto Silva, Flavonoids: prospective drug candidates, Mini Rev. Med. Chem. 8 (2008)

1429–1440.
[19] C. Borsari, N. Santarem, J. Torrado, A.I. Olías, M.J. Corral, C. Baptista, S. Gul, M. Wolf, M. Kuzikov, B. Ellinger, G. Witt, P. Gribbon, J. Reinshagen, P. Linciano, A. Tait, L. Costantino, L.H. Freitas-Junior, C.B. Moraes, P. Bruno Dos Santos, L.M. Alcântara, C.H. Franco, C.D. Bertolacini, V. Fontana, P. Tejera Nevado, J. Clos, J.M. Alunda, A. Cordeiro-da-Silva, S. Ferrari, M.P. Costi, Methoxylated 2'-hydroxychalcones as antiparasitic hit compounds, Eur. J. Med. Chem. 126 (2017) 1129–1135.
[20] C. Borsari, N. Santarem, S. Macedo, M.D. Jiménez-Antón, J.J. Torrado, A.I. Olías-Molero, M.J. Corral, A. Tait, S. Ferrari, L. Costantino, G. Ponterini, S. Gul, M. Kuzikov, B. Ellinger, B. Behrens, J. Reinshagen, J.A. Alunda, A. Cordeiro-da-Silva, M.P. Costi, SAR studies and biological characterization of a 2-(benzo[d][1,3]dioxol-5-yl)-chromen-4-one derivative as a potent anti-trypanosoma brucei agent, ACS Med. Chem. Lett. 10 (2019) 528–533.
[21] J. Baell, M.A. Walters, Chemistry: chemical con artists foil drug discovery, Nature 513 (2014) 481–483.
[22] A. Kerimi, G. Williamson, Differential impact of flavonoids on redox modulation, bioenergetics, and cell signaling in normal and tumor cells: a comprehensive review, Antioxidants Redox Signal. 29 (2018) 1633–1659.
[23] V. Yardley, S.L. Croft, S. De Doncker, J.C. Dujardin, S. Koirala, S. Rijal, C. Miranda, A. Llanos-Cuentas, F. Chappuis, The sensitivity of clinical isolates of Leishmania from Peru and Nepal to miltefosine, Am. J. Trop. Med. Hyg. 73 (2005) 272–275.
[24] E. Bifeld, P. Tejera Nevado, J. Bartsch, J. Eick, J.A. Clos, A versatile qPCR assay to quantify trypanosomatidic infections of host cells and tissues, Med. Microbiol. Immunol. 205 (2016) 449–458.
[25] P. Leprohon, D. Légaré, F. Raymond, E. Madore, G. Hardiman, J. Corbeil, M. Ouellette, Gene expression modulation is associated with gene amplification, supernumerary chromosomes and chromosome loss in antimony-resistant Leishmania infantum, Nucleic Acids Res. 37 (2009) 1387–1399.
[26] F. Dumetz, B. Cuypers, H. Imamura, D. Zander, E. D'Haenens, I. Maes, M.A. Domagalska, J. Clos, J.C. Dujardin, G. De Muylder, Molecular preadaptation to antimony resistance in Leishmania donovani on the Indian subcontinent, mSphere 3 (2018) e00548-17.
[27] K. Choudhury, D. Zander, M. Kube, R. Reinhardt, J. Clos, Identification of a Leishmania infantum gene mediating resistance to miltefosine and SbIII, Int. J. Parasitol. 38 (2008) 1411–1423.
[28] E. Gazanion, C. Fernández-Prada, B. Papadopoulou, P. Leprohon, M. Ouellette, Cos-Seq for high-throughput identification of drug target and resistance mechanisms in the protozoan parasite Leishmania, Proc. Natl. Acad. Sci. U.S.A. 113 (2016) E3012–E3021.
[29] P. Tejera Nevado, E. Bifeld, K. Hohn, J.A. Clos, Telomeric cluster of antimony resistance genes on chromosome 34 of Leishmania infantum, Antimicrob. Agents Chemother. 60 (2016) 5262–5275.
[30] P.C. Melby, B. Chandrasekar, W. Zhao, J.E. Coe, The hamster as a model of human visceral leishmaniasis: progressive disease and impaired generation of nitric oxide in the face of a prominent Th1-like cytokine response, J. Immunol. 166 (2001) 1912–1920.
[31] R. Kumar, S. Nylén, Immunobiology of visceral leishmaniasis, Front. Immunol. 3 (2012) 251.
[32] C. Demicheli, R. Ochoa, J.B.B. da Silva, C.A.B. Falcão, B. Rossi-Bergmann, A.L. de Melo, R.D. Sinisterra, F. Frézard, Oral delivery of meglumine antimoniate–-cyclodextrin complex for treatment of leishmaniasis, Antimicrob. Agents Chemother. 48 (2004) 100–103.
[33] E.E.B. De Paula, F.B. De Sousa, J.C.C. Da Silva, F.R. Fernandes, M.N. Melo, F. Frézard, R.M. Grazul, R.D. Sinisterra, F.C. Machado, Insights into the multi-equilibrium, superstructure system based on -cyclodextrin and a highly water soluble guest β-cyclodextrin and a highly water soluble guest, Int. J. Pharm. 439 (2010) 207–215.
[34] J.M. Requena, M. Soto, M.D. Doria, C. Alonso, Immune and clinical parameters associated with *Leishmania infantum* infection in the golden hamster model, Vet. Immunol. Immunopathol. 76 (2000) 269–281.
[35] M.A. Dea-Ayuela, S. Rama-Íñiguez, J.M. Alunda, F. Bolás-Fernández, Setting new immunobiological parameters in the hamster model of visceral leishmaniasis for in vivo testing of antileishmanial compounds, Vet. Res. Commun. 31 (2007) 703–717.
[36] D. Vanossi, M. Caselli, G. Pavesi, C. Borsari, P. Linciano, M.P. Costi, G. Ponterini, Excited-state intramolecular proton transfer in a bioactive flavonoid provides fluorescence observables for recognizing its engagement with target proteins, Photochem. Photobiol. Sci. (2019), https://doi.org/10.1039/C9PP00026G.
[37] S. Hendrickx, P.J. Guerin, G. Caljon, S.L. Croft, L. Maes, Evaluating drug resistance in visceral leishmaniasis: the challenges, Parasitology 145 (2018) 453–463.
[38] S.L. Croft, K. Seifert, V. Yardley, Current scenario of drug development for leishmaniasis, Indian J. Med. Res. 123 (2006) 399–410.
[39] P.J. Guerin, P. Olliaro, S. Sundar, M. Boelaert, S.L. Croft, P. Desjeux, M.K. Wasunna, A.D. Bryceson, Visceral leishmaniasis: current status of control, diagnosis, and treatment, and a proposed research and development agenda, Lancet Infect. Dis. 2 (2002) 494–501.
[40] K. Katsuno, J.N. Burrows, K. Duncan, R.H. van Huijsduijnen, T. Kaneko, K. Kita, C.E. Mowbray, D. Schmatz, P. Warner, B.T. Slingsby, Hit and lead criteria in drug discovery for infectious diseases of the developing World, Nat. Rev. Drug Discov. 14 (2015) 751–758.
[41] A. Nühs, C. Schäfer, D. Zander, L. Trübe, P. Tejera Nevado, S. Schmidt, J. Arevalo, V. Adaui, L. Maes, J.C. Dujardin, J. Clos, A novel marker, ARM58, confers antimony resistance to Leishmania spp, Int. J. Parasitol. Drugs Drug Resist. 4 (2013) 37–47.
[42] M.C. Laffitte, P. Leprohon, D. Legare, M. Ouellette, Deep-sequencing revealing mutation dynamics in the miltefosine transporter gene in Leishmania infantum selected for miltefosine resistance, Parasitol. Res. 115 (2016) 3699–3703.
[43] F. Di Pisa, G. Landi, L. Dello Iacono, C. Pozzi, C. Borsari, S. Ferrari, M. Santucci, N. Santarem, A. Cordeiro-da-Silva, C.B. Moraes, L.M. Alcantara, V. Fontana, L.H. Freitas-Junior, S. Gul, M. Kuzikov, B. Behrens, I. Pöhner, R.C. Wade, M.P. Costi, S. Mangani, Chroman-4-One derivatives targeting pteridine reductase 1 and showing anti-parasitic activity, Molecules 22 (2017) E426, pii.
[44] C.B. Moraes, M.A. Giardini, H. Kim, C.H. Franco, A.M. Araujo-Junior, S. Schenkman, E. Chatelain, L.H. Freitas-Junior, Nitroheterocyclic compounds are more efficacious than CYP51 inhibitors against Trypanosoma cruzi: implications for Chagas disease drug discovery and development, Sci. Rep. 4 (2014) 4703.
[45] C.B. Moraes, G. Witt, M. Kuzikov, B. Ellinger, T. Calogeropoulou, K.C. Prousis, S. Mangani, F. Di Pisa, G. Landi, L. Dello Iacono, C. Pozzi, L.H. Freitas-Junior, B. dos Santos Pascoalino, C.P. Bertolacini, B. Behrens, O. Keminer, J. Leu, M. Wolf, J. Reinshagen, A. Cordeiro-da-Silva, N. Santarem, A. Venturelli, S. Wrigley, D. Karunakaran, B. Kebede, I. Pöhner, J. Panecka-Hofman, R.C. Wade, M. Fenske, J. Clos, J.M. Alunda, M.J. Corral, E. Uliassi, M.L. Bolognesi, P. Linciano, A. Quotadamo, S. Ferrari, M. Santucci, C. Borsari, M.C. Costi, S. Gul, Accelerating drug discovery efforts for trypanosomatidic infections using an integrated transnational academic drug discovery platform, SLAS Discovery 24 (2019) 346–361.
[46] B. Liu, J. Chang, W.P. Gordon, J. Isbell, Y. Zhou, T. Tuntland, Snapshot PK: a rapid rodent in vivo preclinical screening approach, Drug Discov. Today 13 (2008) 360–367.
[47] M.J. Corral, D.R. Serrano, I. Moreno, J.J. Torrado, M. Domínguez, J.M. Alunda, Efficacy of low doses of amphotericin B plus allicin against experimental visceral leishmaniasis, J. Antimicrob. Chemother. 69 (2014) 3268–3274.